scientific reports

Check for updates

OPEN

Controlling the energies of the single-rotor large wind turbine system using a new controller

Habib Benbouhenni[1]✉, Nicu Bizon[2,3], Ilhami Colak[4], Z. M. S. Elbarbary[5,6] & Saad F. Al-Gahtani[5,6]

In wind energy generation systems, ensuring high energy quality is critical but is often compromised due to the limited performance and durability of conventional regulators. To address this, this work presents a novel controller for managing the machine-side inverter of a single-rotor large wind turbine system using an induction machine-type generator. The proposed controller is designed using proportional, integral, and derivative error-based mechanisms, which fundamentally differ from traditional proportional-integral (PI) regulators. Key features of the proposed regulator include its simplicity, cost-effectiveness, ease of implementation, reduced number of gains, and rapid dynamic response.

This regulator enhances the direct power control (DPC) approach, as it integrates two tailored controllers alongside a pulse width modulation strategy to manage the machine inverter. The DPC strategy incorporating the proposed controller was implemented and tested using MATLAB, with various simulations to evaluate its performance and effectiveness. The proposed regulator demonstrated a significant improvement over the PI regulator, with reductions in active power ripples of 69%, 61.70%, and 59.14% across different tests. Additionally, the steady-state error of reactive power was reduced by 54.84%, 85.23%, and 62.68%, and the total harmonic distortion of current decreased by 48.12%, 50.55%, and 56.05%. These results underscore the high efficiency, robustness, and effectiveness of the proposed controller in improving system performance compared to conventional PI regulators. The controller's outstanding performance makes it a promising solution for broader industrial applications.

Keywords Single-rotor large wind turbine system, Direct power control approach, Induction generator, Pulse width modulation

Abbreviations

PI	Proportional-integral controller
WS	Wind speed
PQ	Power quality
DFIG	Doubly-fed induction generator
ES	Energy system
THD	Total harmonic distortion
DR	Dynamique response
FL	Fuzzy logic
DPC	Direct power control
Ps	Active power
SRLWT	Single-rotor large wind turbine
RSC	Rotor side converter
IG	Induction generator

[1]Department of Electrical Engineering, LAAS laboratory, National Polytechnic School of Oran- Maurice Audin, Oran El M'naouer 1523, BP, Algeria. [2]The National University of Science and Technology POLITEHNICA Bucharest, Pitești University Centre, Pitesti 110040, Romania. [3]ICSI Energy, National Research and Development Institute for Cryogenic and Isotopic Technologies, Ramnicu Valcea 240050, Romania. [4]Istinye University, Istanbul, Turkey. [5]Department of Electrical Engineering, College of Engineering, King Khalid University, P.O. Box 394, Abha 61421, KSA, Saudi Arabia. [6]Center for Engineering and Technology Innovations, King Khalid University, Abha 61421, Saudi Arabia. ✉email: habib.benbouhenni@enp-oran.dz

GSC	Grid side converter
PSO	Particle swarm optimization
GWO	Grey wolf optimization
MPPT	Maximum power point tracking
SMC	Sliding mode control
SOSMC	Second-order sliding mode control
SSE	Steady-state error
IOPI	Integer-order proportional-integral controller
FOPI	Fractional-order proportional-integral controller
Qs	Reactive power
MM	Mathematical model

In energy systems (ESs), the controls used are largely responsible for power quality (PQ), complexity, dynamic response (DR), and ease of operation. Therefore, it is necessary to pay attention to these controls and try to improve their performance and durability. These regulators are multiple, as the proportional-integral (PI) approach is considered one of the most famous of these regulators in the area of control and electronics[1]. This regulator is simple, low in cost, has a low number of gains, and is easy to implement[2]. All these features make this regulator the most reliable solution. Despite this performance, this regulator is characterized by a negative, represented by a decrease in competence in the event of a flaw in the system, which allows for a decrease in PQ, as demonstrated by the work done in[3].

To avoid this problem and to raise the fineness of power resulting from ESs, many new controllers have been proposed, such as sliding mode controller (SMC)[4], passivity regulator[5], backstepping controller (BC)[6], and active disturbance rejection control (ADRC) strategy[7]. These controllers are described by high robustness, high efficiency, and great competence in enhancing the features of ESs. However, the use of these controllers has disadvantages, namely the high level of complexity, costs, and their dependence on the mathematical model (MM) of the ES, which causes a decrease in the fineness of energy and stream in the event of a flaw in the ES[8,9]. Also, the use of these regulators does not eliminate power fluctuations, as ripples are observed at the level of energy, torque, and stream, as demonstrated by research works[10–12]. In[13], it was proposed to use non-linear control to control doubly-fed induction generator (DFIG) powers. The use of this proposed strategy aims to improve the performance, stability, and robustness of the studied ES. This proposed control is an adaptive nonlinear back-off control based on the Lyapunov function. This designed algorithm is used to control the electromagnetic torque of the generator while keeping the reactive stator power equal to zero. This designed approach allows the maximum power point (MPP) to be extracted, despite wind speed (WS) variations. The designed algorithm was realized in a MATLAB simulation environment, comparing the results to the traditional approach. The results show that using this algorithm increases the robustness and performance of the studied system and increases the DFIG power quality. Using this designed algorithm has disadvantages that lie in its reliance on power estimation, which makes it affected by changes in system parameters. Also, using this designed algorithm requires knowing the exact MM of the machine, which is not desirable. Another nonlinear strategy proposed in[14] is to combine SMC and BC to control the power of an ES based on the use of DFIG. This strategy was only applied to the machine inverter without the grid inverter. The proposed strategy is characterized by high robustness and great ability to improve PQ, as shown by simulation results. This proposed strategy is used to find the reference value of the effort. These voltage reference values (VRVs) are converted by the pulse width modulation (PWM) strategy into pulses to operate the DFIG inverter. The use of this strategy is based on the use of power estimation. Variable WS was used to study the efficiency, effectiveness, and ability of this strategy to improve the PQ of DFIG. The simulation results showed the effectiveness of the combination SMC and BC in improving PQ, total harmonic distortion (THD) value, and power response time (RT) compared to the traditional approach and some existing works. Despite this performance provided by the designed strategy, some drawbacks limit its spread and use in the field of control. The most prominent of these disadvantages are complexity, expense, difficulty in control due to a significant number of gains, and difficulty in completion. In the work[15], two different controllers were proposed to overcome the problem of low PQ and high THD current for an ES based on the use of DFIG. These two controllers are the SMC and BC approaches, as they are characterized by high durability and distinctive performance compared to the PI approach. Using these two controllers requires knowledge of the MM of the DFIG. The strategy was applied to the DFIG inverter only, where space vector modulation (SVM) was used to convert the VRVs generated by both the SMC and BC approaches into pulses to drive the DFIG inverter. In this work, variable WS was used to study the effectiveness, efficiency, and robustness of the two approaches. After giving MMs for each approach, these strategies were implemented using MATLAB. In all tests performed, the SMC approach strategy provided satisfactory results compared to the BC approach regarding reduced power ripple, current THD value, overshoot, and DFIG power steady-state error (SSE). However, in the robustness test, it is noted that the two approaches were affected by significantly changing DFIG parameter values, which is undesirable. The phenomenon of chattering is one of the most prominent drawbacks of using the SMC approach, which limits its spread. Also, the BC approach is characterized by its complexity and the presence of a significant number of gains, which limits its use and spread in the control field. A simple and easy-to-implement strategy was used in[16] to continuously and independently control the reactive and active power (*Qs* and *Ps*) generated by a DFIG of a flow-directed wind ES. This strategy relies on fuzzy logic (FL) that does not require knowledge of the MM of the machine. The use of the FL algorithm depends largely on experience, and its use allows for a significant increase in performance and durability. This designed control was applied to the DFIG inverter, where MATLAB was used to implement it. A variable WS was used and a comparison study was conducted with the traditional approach. The obtained results highlight the superiority of the FL approach over the traditional approach in terms of improving reference tracking, reducing energy ripples, overshoot value, and

THD of current. However, the use of the FL approach has drawbacks that limit its use, as there is no rule to help choose the best number of rules to obtain satisfactory results. Also, using a larger number of rules makes the system slower, which is not desirable. The fractional-order proportional-integral-derivative (FOPID) controller is an efficient and simple solution proposed in[17] to improve the PQ and reduce the THD of DFIG current. This controller is simple and easy to implement. The FOPID controller was used to control the torque and flux of the DFIG. This controller is used to find VRVs, and these reference values are used to generate the pulses necessary to operate the machine's inverter. Using a FOPID controller reduced power ripples and significantly improved the THD value compared to using a PI controller. However, using a FOPID controller has its drawbacks, which include a large number of gains compared to a conventional controller. Also, the use of the FOPID controller is affected by changes in DFIG parameters, as shown by the robustness test, which is negative.

To obtain strong competence and great efficiency in ESs, the regulator used must be characterized by several features, including simplicity, high durability, low costs, high efficiency, fast DR, and, most importantly, it does not require information on the MM of the ES under study. In the work[18], it was proposed to use an indirect field-oriented control (IFOC) strategy based on artificial intelligence (AI) to control the capabilities of a squirrel-cage induction generator. The AI approach was used to overcome the disadvantages of the IFOC strategy, as all controls were compensated Also, in this work, we relied on estimating the speed of the rotating part to obtain distinctive and effective performance. This proposed approach was implemented experimentally using real tools, where the experimental results showed the effectiveness and efficiency of using an AI controller in improving the quality of power and current compared to a PI regulator. Despite this performance, the problem of ripples remains present in the proposed approach, as it is observed that the ripples and THD of current increase, especially in the event of a change in the DFIG parameters. A simple strategy has been proposed to regulate the flow of *Ps* and *Qs* in[19] based on the use of a neural tuning machine (NTM) built on a recurrent neural network. In this work, the focus is on controlling the *Qs* flow from the rotor-side converter (RSC), which is proportional to the grid-side controller (GSC) through coupling voltage. The proposed NTM method leverages neural networks (NNs) to adjust PI controller parameters and improves the performance of DFIG network integration. Using the designed strategy allows for increased robustness, enhanced adaptability, and nonlinear dynamics, thus addressing network challenges. Also, this algorithm designed for voltage regulation was used. The advantages of the neural tuning machine in controlling internal current loop parameters are highlighted with results compared to conventional PI regulators, where a MATLAB/Simulink model is modeled using three different measurement models. The simulation results highlight the effectiveness and strength of the designed approach in improving PQ and increasing durability compared to using a traditional PI regulator. Despite this effectiveness, there are drawbacks to using this designed algorithm. These drawbacks lie in the use of NNs, as no rule facilitates adjusting the number of internal layers needed to obtain better results. In the work[20], a simple controller based on the use of a fractional-order PI regulator based on particle swarm optimization (PSO) was proposed to control the powers of the DFIG in the presence of various faults. As known, studying power grid faults is crucial to maintaining grid reliability and stability. Understanding these faults allows rapid detection, prevention, and mitigation of their effects, ensuring uninterrupted electricity supply, protecting equipment, and preventing potential cascading faults, which reduces regular maintenance costs. In addition to using the FOPI-PSO controller, symmetrical fault-tolerance control techniques (SFRT) and asymmetric fault-to-pass control techniques (AFRT) are implemented to improve performance and efficiency. These technologies play a pivotal role in maintaining the stability and reliability of the ES during difficult and complex conditions. The proposed approach aims to improve the performance of RSC under error conditions. A comparative study was performed between the proposed approach and the traditional approach to demonstrate the potential advantages and limitations of the new control technology, which contributes to the development of error mitigation strategies in wind turbine systems. Also, the economic feasibility of the proposed control method and its suitability to address wind farm issues such as PQ were highlighted. In addition to using the FOPI-PSO controller, SFRT and AFRT are implemented to improve performance and efficiency. These technologies play a pivotal role in maintaining the stability and reliability of the ES during difficult and complex conditions. The proposed approach aims to improve the performance of RSC under error conditions.

Nonlinear model predictive command is an approach proposed in[21] to control the IG, where variable WS was used to complete this study. This proposed approach was compared with PI control, where the Lyapunov theory was used to study the stability of the designed approach. MATLAB was used to achieve this control and verify its durability and performance. All results indicate the high performance that characterized this approach in terms of PQ and robustness compared to the PI control. However, this proposed approach has disadvantages that include complexity, a large number of gains, unsatisfactory DR compared to PI control, and difficulty of implementation. Also, despite the performance, undulations are observed at both the stream and energy levels, which is undesirable. In[22], a hybrid cascade FL-PI approach was used to command the IG. This designed approach is based on experience and does not require information on the MM of the ES, which makes it perform highly in the event of an ES flaw. This approach was realized in MATLAB, where a variable WS was used. The results obtained show the extent of the competence, durability, and efficiency of this approach in ameliorating the fineness of stream and power compared to the usual competence. The negative of this proposed approach lies in the number of FL rules required to obtain good results, as there is no mathematical rule that determines the best number. According to the work[23], the use of a fractional-order PI regulator leads to a significant enhancement in the fineness of stream and power compared to a traditional controller. Also, using this regulator contributes to greatly raising the durability of the ES. However, using this regulator does not lead to overcoming the problem of power undulations, as the undulations remain present, which is a negative thing. In[24] a new control was used based on the use of a PI controller based on smart strategies to control the powers of DFIG. Both grey wolf optimizer (GWO) and whale optimization algorithm were used to improve the characteristics of the PI controller. Using these smart strategies allows us to improve the PQ significantly. Simplicity, high

durability, ease of implementation, and DR speed are the most notable features of this designed controller. This proposed strategy was implemented on a machine inverter and a grid inverter for an ES consisting of a 6 MW wind farm. Smart strategies were used to determine the gain values of the PI controller. MATLAB was used to implement the designed algorithm and compare it with the traditional approach. The results obtained showed the effectiveness of the PI controller based on smart strategies in increasing durability, efficiency, and reducing power fluctuations compared to the traditional controller. Also, reduced THD value compared to the traditional strategy. This designed strategy has disadvantages that lie in its being affected by changing machine parameters, which is undesirable. An FL-PI controller was relied upon to control the power of the DFIG[25]. Using the FL-PI controller does not require knowledge of the MMM of the DFIG, which makes it easy to implement. The FL-PI controller is characterized by simplicity, fast DR, and ease of operation. This proposed strategy was applied to the inverter DFIG only to prove its effectiveness and robustness in improving the quality of power and current without the need to control the GSC. Also, the FL approach was used to improve the effectiveness and efficiency of the MPP tracking (MPPT) approach. The FL-MPPT approach is used to determine the reference value for *Ps*, and therefore the value of current and torque are related to the form of WS change. MATLAB was used to verify the safety and robustness of the proposed method under different working conditions while comparing the results with the traditional method. In all tests, the designed method provided satisfactory results compared to the traditional method in terms of reference tracking, PQ, and THD value of the current. This proposed algorithm has drawbacks that limit its spread, no rule facilitates the use of the FL approach to obtain excellent results. The use of the FL approach depends largely on experience and experimentation in determining the appropriate number of rules, which requires a lot of time and effort. In[26], a newly developed social spider optimization (SSO) technique is used to optimize the design parameters of fuzzy proportional integral with derivative (FOFPID) to improve the performance and effectiveness of direct vector control (DVC). DVC is an easy-to-implement, fast DR, and robust and widely used energy control strategy. This strategy can be relied upon to deal with winds that vary quickly and randomly. Using this designed strategy allows for maintaining the output power of the studied DFIG-based WTS at the rated value under dynamic wind conditions. To increase efficiency and performance, the proposed FOFPID controller integrates the capabilities of the FL smart regulator and the fractional-order controller while allowing independent control of *Ps* and *Qs*. This designed algorithm was applied to RSC, where it was used to replace the traditional PI regulator in the internal current loops of the traditional approach. MATLAB was used to implement this designed algorithm with extensive evaluations of performance under various operating conditions, including active reference power changes, parameter uncertainties, and rapid WS changes. Comparative analyses with PID and SSO-enhanced fuzzy regulators show that the FOFPID regulator performs better in terms of maximum overshoot, extreme undershoot, settling time, THD, and weighted THD (WTHD). The proposed FOFPID regulator also displays stronger robustness against parameter mismatch and weather variation compared to other regulatory architectures. The disadvantage of this designed approach lies in its complexity and the presence of a significant number of gains, which makes it difficult to adjust the DR.

Non-singular terminal SMC and double interval type-2 FL systems are combined into work[27] to control the IG. This designed approach relies on two different controls, which makes it highly robust and has distinctive competence compared to the usual approach. This designed approach was realized using a Real-Time Model in Loop (RT-MiL), with results compared to the usual approach. The experimental results showed that this approach is described by great competence and durability compared to the usual control, as the undulations were significantly reduced. Despite this competence, this approach has negatives that lie in its complexity, the difficulty of completion, the presence of a significant number of gains, and the DR that is not satisfactory compared to PI control. In the work[28], adaptive FL extended state observer and SMC approach were used to control the power. In this work, several smart strategies were applied to calculate the values of the designed control parameters. Thermal exchange optimization (TEO), GA, PSO, water cycle approach (WCA), harmony search approach (HSA), and grasshopper optimization approach (GOA) were used. Also, in this work, a comparison was made between the TEO-tuned PI regulator, the TEO-tuned STA-second-order sliding mode (SOSM) approach, and STA-SOSM approach-based linear observer, where MATLAB was used for this purpose. Results show that using the TEO approach leads to ameliorating the features of the controllers well while reducing power and current ripples. In[29], a nonlinear control was proposed for a generator with a power of 100 MW, where variable-gain super-twisting SMC damping control was used for this purpose. Also, MPPT approach was used to calculate current reference values. This designed approach is described by high competence and great efficiency, as the energy change is related to the change in WS as a result of using the MPPT approach. This approach was compared with the PI control, partial feedback linearization control, and first-order SMC, where MATLAB was used for this purpose. All obtained results show the superiority of the designed approach over other approaches in terms of stream and PQ. Also, this proposed approach provided very satisfactory results in terms of overshoot value, and THD of stream. Voltage modulated direct power control (DPC) approach has been proposed to control IG[30]. This approach differs from the traditional DPC approach in terms of competence and robustness. This approach was suggested to beat the cons of power fluctuations and augmentation of the robustness of the control ES. However, this approach has drawbacks that lie in its complexity, the presence of a significant number of gains, and the difficulty of realization. Results obtained from MATLAB show the high competence of this designed approach compared to DPC in terms of PQ and THD of the stream. From the results presented, it is noted that fluctuations remain present at the level of current, torque, and energy, which is negative. It is also observed in the durability test that this designed approach is significantly affected as a result of its reliance on the MM of the machine. In[31], DPC based on the SOSM approach was used to control the IG energy. To calculate the designed control parameters, the TEO was used for this purpose. This designed approach is described by high efficacy and outstanding competence, and this is shown by the results from MATLAB. Also, this proposed strategy reduced the chattering phenomenon significantly, which shows its high performance.

FL approach and second-order SMC (SOSMC) technique were combined to overcome the problems of the DPC strategy and improve the PQ generated by DFIG[32]. The FL-SMC strategy is characterized by high durability and outstanding performance, as a control was used to control the power of the DFIG. The FL-SOSMC controller was used to convert power errors to VRVs. These reference values are converted into pulses using the SVM strategy. Also, the FL-SOSMC controller was used to control the power of the DFIG inverter only. MATLAB was used to implement the designed method and compare it with the traditional method in terms of reducing ripples and the THD value of the current. Variable WS was used to complete this study. The presented results showed that the FL-SOSMC controller gave a distinctive performance in terms of reducing power ripples and the THD value of the current compared to the traditional method. This designed FL-SOSMC controller also gave satisfactory results in the durability test compared to the PI controller, although it was affected. In[33], three different controls are used to control the power of the DFIG. These controls are FL-SMC approach, SOSMC approach, and integral BC technique. These controllers were proposed to control both the RSC and the GSC. These strategies were proposed to overcome the problems and drawbacks of the vector control strategy based on the PI controller. The author in[34] proposed a control based on the use of fractional-order PID and GWO algorithms to improve the quality of power generated by a DFIG-based ES. This strategy has a great ability to reduce power ripples, current, and torque compared to using a traditional controller. In this designed strategy, the GWO algorithm was used to calculate the FOPID controller gain values. The FOPID controller is used to determine VRVs. This designed approach was tested in the case of variable WS using MATLAB. The completed tests showed the significant superiority of the designer's method compared to the traditional approach in terms of improving PQ compared to the traditional method. The main purpose of the proposed control strategies is to maintain the stable operation of the DFIG and its transformers during internal and external uncertainties. Also, the PWM strategy was used to generate the pulses needed to operate both the RSC and GSC. These strategies were implemented using MATLAB/SIMULINK environment. The simulation results obtained in this work demonstrate the robustness of each control strategy compared to a conventional controller despite different disturbances and uncertainties. The author in[35] replaced the PI of field-oriented control used to control the DFIG-based wind turbine with NN controllers. The use of PI based on neural algorithm allows for improving the characteristics of the user control and thus the PQ. Despite the outstanding performance, the problem of power ripples remains present, especially in the durability test. A noticeable increase in power ripples and a decrease in the quality of the current are noted. This is due to the use of an approach designed for the MM of the machine, which is a negative. In addition, the designed strategy relies on estimating powers, which increases its impact on changing DFIG parameters. The PI controller is the simplest solution that can be relied upon due to its fast DR and ease of implementation. However, its use causes several disadvantages, especially in ESs based on renewable sources. Therefore, the author in[36] used controllers represented by RST and ADRC and compared them to the PI controller to find out which strategy gives a higher PQ to a turbine system. These strategies have common features, which are characterized by simplicity, ease of implementation, and fast DR. These strategies were used to control the power of DFIG. These strategies were implemented in a MATLAB environment using variable WS. The simulation results showed that RST and ADRC are superior to the traditional PI controller in terms of SSE, rise time, overshoot, and settling time values. In the robustness test, it was noted that the RST and ADRC strategies are less affected by changes in machine parameters compared to the PI controller, with an advantage for RST in terms of rise time. A comparison was proposed between two different controls in terms of their ability to improve the PQ of an energy system based on the use of a wind turbine[37]. These two controls are the artificial neural network (ANN) control and the PI regulator, which were used to control the DFIG power. First, an MM was given for each controller, mentioning the pros and cons. Secondly, these controls were implemented using MATLAB, where two different WS profiles were used to compare performance. Simulation results showed that using an ANN controller gives greater percentages of power fluctuation reduction and current THD than the PI regulator. However, it is noted in the robustness test that the PI strategy was greatly affected by the change in DFIG parameters compared to the ANN-based control. This effect appears by increasing the power ripple value and THD current value. From reviewing the above literature and works, there is no powerful controller that is simple and easy to implement, so the search for the best controller continues.

Adaptive-higher-order sliding mode (AHOSM) is a control approach proposed in[38] for control in IG, and MATLAB was used to realize it. This designed approach is based on the MM of the IG and is described by high robustness compared to the usual control based on the PI regulator. This approach is based on the Lyapunov function, which makes it provides high competence in minimizing energy undulations and the THD of the stream. The results were compared with both the PI control and the usual first-order SMC, and a comparison showed the superiority of the designed method over these controls. Despite this superiority, the drawback of energy and stream fluctuations remains. Also, in the durability test, it is noted that this suggested approach is affected by changing generator parameters, which is negative. In[39], an integer-order PI (IOPI) was used to control the power of the IG in the tidal stream turbine system. The control approach is characterized by high performance, simple, easy to realize, uncomplicated, and highly durable. This designed regulator was compared with a fractional-order PI (FOPI), where MATLAB was used for this purpose. The use of a FOPI regulator led to enhanced dynamic power response, reduced energy undulations, and reduced SSE value compared to an IOPI regulator. However, the problem of the fineness of stream and power remains present in this designed approach, as it is observed that it decreases if the IG parameters are changed. In[40], the TEO was used to estimate the values of the PI parameters of the IG generator. Using this approach led to a significant enhancement in the fineness of stream and energy. The results showed that using this approach significantly improved the DR compared to the PI. This approach has a negative effect that lies in energy fluctuations, as special fluctuations are observed in the robustness test, which is negative.

In this research, a new controller is applied for both *Qs* and *Ps* generated by IG-based single-rotor large wind turbine (SRLWT) systems. This controller is designed based on proportional, integral, and derivative actions of

the error. Simplicity, fast DR, ease of realization, small number of gains, and low cost are the most prominent features of this proposed regulator. Therefore, this proposed controller is considered the main contribution of this paper. First, this designed regulator was used to overcome the problems and defects of the DPC strategy of DFIG-SWRWT system. Therefore, the DPC strategy based on the designed regulator is the second main contribution of the paper. The ES proposed in this study is based on the use of an SRLWT turbine. Using this turbine to convert wind energy into mechanical energy makes the work done different from the work found in the literature. Therefore, this turbine is the third major contribution of this paper. DPC strategy based on the designed regulator is a development of the traditional strategy, where the PWM strategy was used to generate the necessary pulses based on the voltage reference values. This strategy uses the same estimation equations used in the traditional strategy. To implement this strategy, MATLAB was used with two different WS profiles to study the effectiveness and strength of this designed strategy. All tests showed the high performance of this strategy, making it a reliable solution in industrial applications in the future.

The objectives achieved by this work are the following points:

- Overcoming the disadvantages of the DPC of DFIG strategy.
- Improve the quality of power and current.
- Overcoming the disadvantages of PI controller.
- Significantly increasing the durability of the control system.
- Significantly improved value compared to traditional controllers and some works.
- Significantly improve the overshoot value compared to the traditional approach.
- Reducing the SSE of IG power.

Accordingly, the completed work was divided into six different sections. The second section presented the ES proposed for the study, where the mathematical modeling of the main elements composing this system was discussed, mentioning the negatives and positives. After that, the third section presented the designed controller, where its features and MM were discussed. In the fourth section, the application of the controller designed to control the powers of the IG-SRLWT is discussed, and the necessary information is given. The fifth section implements the controller designed in MATLAB and compares its performance with the traditional controller. Also, the results are compared to several published scientific works. Finally, all the conclusions obtained in this work are collected in Section VI with future work given as a sequel to this work.

Proposed power system

To augment the energy gained from the wind, an SRLWT is used. The use of one of these WTs contributes to raising the robustness and stability of the studied ES, as this proposed ES relies on the use of an IG generator. This generator uses a 2-level inverter to feed it from the network. The PWM approach is used to run the inverter of the machine, as this approach is described by simplicity, ease of realization, and low charge.

Figure 1 represents the ES proposed for study in this work. The use of this designed ES contributes significantly to minimizing the use of non-renewable energy sources and minimizing the phenomenon of global warming. So, the use of this ES contributes greatly to protecting the environment. This ES has advantages such as simplicity, ease of implementation, inexpensive, and does not require complex control. This proposed ES can be used at the individual level, which allows it to beat the problem of the increasing energy demand. Also, this proposed ES allows for minimizing the charges of creating and consuming electrical power.

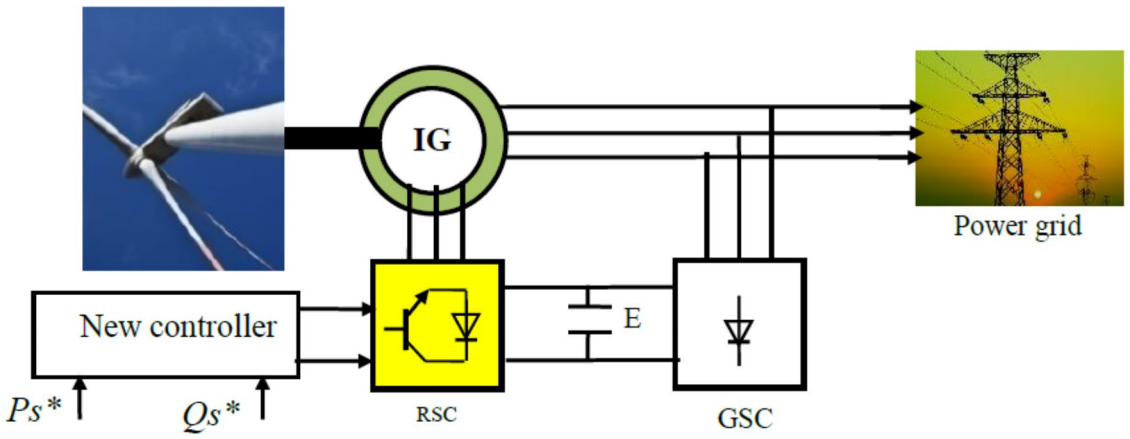

Fig. 1. Designed ES.

SRLWT model

The SRLWT is considered one of the most important components of the proposed ES station, as this turbine is responsible for generating energy from wind. The use of this turbine allows for overcoming the phenomenon of global warming and reduces dependence on traditional energy sources. Also, the use of these turbines allows for overcoming energy demand and reducing the energy production and consumption bill[41]. Turbines are considered an effective solution for generating energy for non-petroleum governments, as they can be used on land and at sea. Demand for wind turbines in European countries increased by 74% in 2020, reaching a record high of 15 gigawatts. This percentage indicates the energy transformation taking place across European countries and the extent of their dependence on the use of non-renewable energy sources to generate electrical energy. Also, the percentage of demand for onshore wind turbines in European countries amounted to 8.2 gigawatts, an increase of 13% compared to 2019. As for foreign orders for wind turbines in 2020, they increased six-fold compared to 2019 to reach 6.4 gigawatts. Several turbines are used in the form of farms called wind farms. The larger the number of turbines used in wind farms, the greater the energy produced[42]. The power produced by turbines depends on the WS and the size of the turbine. The larger the turbine dimensions, the greater the energy produced. A turbine with three blades is often used because it generates more energy from the wind compared to a wind turbine with one or two blades.

The energy gained from wind using a turbine is expressed by Eq. (1). This gained energy (P_t) is affected by a factor called the coefficient of power (Cp), whose value does not exceed 1[43].

$$P_t = \frac{1}{2}\rho\, R^2 C_p\,(\beta\,,\ \lambda\,)\, V^3 \tag{1}$$

Where, V is the speed of wind, ρ is the Air density, and R is the blade radius.

The turbine torque can be calculated from the gained energy, as Eq. (2) is used to calculate it.

$$T_{aer} = \frac{1}{2\Omega_{\,t}}\rho\, R^2 C_p\,(\beta\,,\ \lambda\,)\, V^3 \tag{2}$$

Where, T_{aer} is the aerodynamic torque, and Ω_t is the turbine speed.

The value of the Cp factor is affected by the blade angle (β) and the tip speed ratio (λ), where the largest value of this factor is when the blade angle value is equal to 0 degrees. This is a coefficient that can be calculated according to the work[44] using the Eq. (3).

$$C_p(\lambda\,,\ \beta\,) = \frac{46}{100}\left(\frac{151}{\lambda_{\,i}} - \frac{58}{100}\beta\ - \frac{2}{1000}\beta^{\,2.14} - 13.2\right) e^{\frac{-18.4}{\lambda_{\,i}}} \tag{3}$$

The value of λ is related to the WS, as the greater the wind speed, the lower the value of λ and vice versa. The value of λ is also affected by the speed of the turbine, as the greater the speed of the turbine, the greater the value of λ. The blade length of the turbine greatly affects the value of λ. The longer the blade, the larger the value of λ. Equation (4) is used to calculate the value of λ.

$$\lambda\ = \frac{\Omega_{\,t}}{V} R \tag{4}$$

In an energy system based on wind turbines, the rotational speed of the turbine is less than the rotational speed of the generator. Therefore, a gearbox is used. This gearbox is used to increase the speed of the turbine to obtain the necessary speed for the generator. Equation (5) is used to calculate the speed and torque of the generator based on the speed and torque of the turbine[45].

$$\begin{cases} T_{aer} = T_m.G \\ \Omega_{\,m} = G\Omega_{\,t} \end{cases} \tag{5}$$

To control the turbine, the MPPT strategy is used. This strategy is characterized by simplicity, ease of implementation, uncomplicated, and quick DR. This strategy relies on the use of the PI regulator, as it has been detailed in several different works[46–48]. Using the MPPT strategy allows the energy gained from the wind to be related to the change in WS.

RSC model

The strategy designed in this work is used to control RSC. The use of RSC by a two-level inverter is proposed to reduce costs, simplify the system, simplify control, and demonstrate how the designed controller can improve power and current accuracy. The GSC is used by an uncontrolled inverter to simplify the studied ES, simplify control, and reduce costs. Also, to show how powerful the designed approach is in improving the quality of power and current without resorting to GSC control. To generate the pulses needed to operate the RSC, a PWM method is used that converts voltage reference values into pulses. The PWM strategy is characterized by simplicity, ease of control, low costs, and ease of experimental realization. A two-level reflector has been modeled in several different works[49,50]. According to these works, the MM of a two-level reflector can be represented by Eq. (6).

$$\begin{bmatrix} V_a \\ V_b \\ V_c \end{bmatrix} = \frac{E}{6}\begin{bmatrix} 2 & -1 & -1 \\ -1 & 2 & -1 \\ -1 & -1 & 2 \end{bmatrix}\begin{bmatrix} F_1 \\ F_2 \\ F_3 \end{bmatrix} \tag{6}$$

Where, F_1, F_2, and F_3 they are values that can take the value 1 or -1, depending on the condition of the transistors.

IG model

Induction machines are among the most famous and widely used machines in industrial fields. These machines have many advantages such as low cost, little maintenance, high durability, and ease of control. These induction machines can be used in the field of renewable energies to generate electrical energy. According to the work done in[51], induction machines have a high ability to operate in variable WS conditions compared to other machines[52,53]. The mathematical modeling of this machine is based on the use of the Park transformation, where the parts of the machine are represented by mathematical equations. In this work, a DFIG-type IG was used. This type allows controlling the generated power based on controlling the feeding of the rotor. This feature makes this type more effective and efficient in the case of variable WS. Machine powers can be calculated using Eq. (7). The power of a machine is related to current and voltage, as depending on the current absorbed by the machine, the torque and power generated by this machine can be controlled.

$$\begin{cases} P_s = \frac{3}{2}(+V_{qs}I_{qs} + V_{ds}I_{ds}) \\ Q_s = \frac{3}{2}(+V_{qs}I_{ds} - V_{ds}I_{qs}) \end{cases} \tag{7}$$

Equation (8) expresses both the flux and voltage of the stator part of the machine[51].

$$\begin{cases} V_{ds} = R_s I_{ds} + \frac{d}{dt}\Psi_{sd} - w_s \Psi_{qs} \\ \Psi_{ds} = L_s I_{ds} + M I_{dr} \\ V_{qs} = R_s I_{qs} + \frac{d}{dt}\Psi_{qs} + w_s \Psi_{ds} \\ \Psi_{qs} = L_s I_{qs} + M I_{qr} \end{cases} \tag{8}$$

Where, R_s is the stator resistance, V_{qs} and V_{ds} are the stator voltages in the *d-q* reference frame, L_s is the stator inductance, and Ψ_{qr} and Ψ_{dr} are the rotor flux in the *d-q* reference frame.

The rotor voltage is linked to the stream, and its value can be determined using Eq. (9). Using Eq. (9), the flux value for this part of the machine can be calculated. The flux of the rotor part can be changed by current control[53].

$$\begin{cases} V_{dr} = R_r I_{dr} + \frac{d}{dt}\Psi_{dr} - w_r \Psi_{qr} \\ \Psi_{dr} = L_r I_{dr} + M I_{ds} \\ V_{qr} = R_r I_{qr} + \frac{d}{dt}\Psi_{qr} + w_r \Psi_{dr} \\ \Psi_{qr} = L_r I_{qr} + M I_{qs} \end{cases} \tag{9}$$

Where, V_{qr} and V_{dr} are the rotor voltages in the *d-q* reference frame, Ψ_{qr} and Ψ_{dr} are the rotor flux in the *d-q* reference frame, L_r is the rotor inductance, M is the mutual inductance, and R_r is the rotor resistance.

The expression for torque is included in Eq. (10), where the expression for this torque is linked to the development of the speed of the machine. This equation is of great importance, as though it is possible to control the operation of this machine, either a generator or a motor.

$$\begin{cases} T_e - T_r = f\Omega + J\frac{d\Omega}{dt} \\ T_e = \frac{3}{2}p\frac{M}{L_s}(\Psi_{sq} I_{rd} - \Psi_{sd} I_{rq}) \end{cases} \tag{10}$$

Where, *Te* is the torque generator, I_{qr} and I_{dr} are the rotor currents in the *d-q* reference frame, Ω is the speed of generator, p is the number of pole pairs, and *f* is the viscous friction.

A study of the literature indicates that many different controllers have been proposed to control IG force, such as PI regulator, backstepping controller, synergetic controller, and STC regulator. These controls vary in terms of complexity, difficulty of implementation, efficiency, efficiency, and performance. Some of these controllers give good results, but they are complex and the DR is difficult to adjust. Some control approaches depend on the MM of the machine, which makes them affected by changes in the machine parameters. Therefore, in the next part, a regulator is proposed that features strong performance, fast DR, and ease of implementation.

Proposed controller

In this part, the controller's proposal is characterized by simplicity and ease of realization. This proposed controller differs from the controllers found in the literature, as the structure of this controller depends on proportional, integral, and derivative error procedures.

As is known, the PI controller is characterized by fast DR and easy adjustment. Also, the PD-type controller is characterized by simplicity, few gains, and ease of operation. Applying both PD and PI does not require knowledge of the MM of the machine.

In Eqs. (11) and (12) the MM for both PI and PD is given.

$$u(t) = K_1 e(t) + K_2 \int e(t)\, dt \tag{11}$$

$$w(t) = K_3 e(t) + K_4 \frac{de(t)}{dt} \tag{12}$$

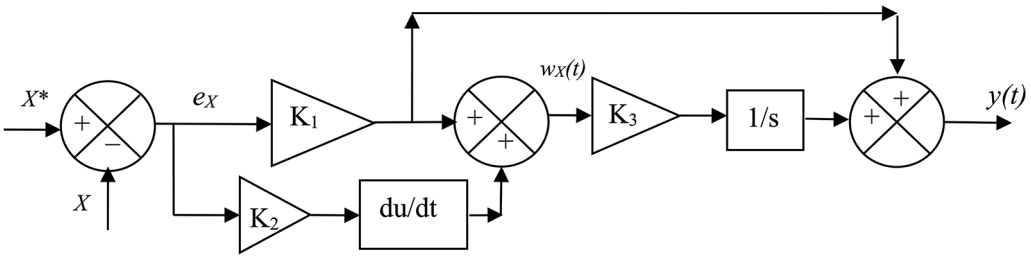

Fig. 2. Proposed controller.

Features	Proposed controller	SMC	Synergetic controller	Backstepping controller	Predictive controller
Simplicity	Yes	No	Yes	No	No
Number of gains	Low	Medium	Low	High	High
Affected by changing machine parameters	Low	High	Low	High	High
Performance	High	High	High	High	High
Durability	High	High	High	High	High
Application to complex systems	Easy	Complicated	Easy	Complicated	Complicated
Use a MM of the machine	No	Yes	No	Yes	Yes
Ease of completion	Yes	No	Yes	No	No
DR	Very fast	Fast	Very fast	Fast	Fast

Table 1. Comparing the designed controller with some existing controllers.

Despite the advantages of PD and PI, their use in the field of renewable energies gives unsatisfactory results in terms of PQ and THD of current, especially in the event of a malfunction in the automated system. To overcome this problem, several solutions were used, including PD(1 + PI)[54] and PI(1 + PI)[55]. Using these two solutions gave satisfactory results in terms of increasing PQ. However, these proposed solutions have drawbacks, the most prominent of which is complexity and difficulty in control due to the presence of a significant number of gains.

To overcome the problem of complexity and difficulty of adjustment, a new controller is proposed that is completely different from the controllers found in the literature. This controller designed as an effective and convenient solution is represented in Fig. 2. This figure gives a clear picture of how simple and easy it is to adjust this designed regulator.

According to Fig. 2, the designed regulator does not need to know the MM of the machine compared to many other controllers such as SMC, which makes this designed regulator one of the most reliable solutions in the future. Also, its use does not require complex calculations, which makes it a suitable solution for complex and large systems.

Equation (13) represents the MM of the regulator designed in this paper, which will be used in the next section to control power.

$$y(t) = (K_1 e_x(t) + K_2 \frac{de_x(t)}{dt})(K_3 \int w(t)\,dt) + K_1 e_x(t) \tag{13}$$

Where, K_1, K_2, and K_3 are the gains of the proposed new regulator. Using the values of these gains, the DR can be adjusted to obtain the desired performance.

Gain values for this designed controller can be calculated using intelligent strategies such as GA. However, using these strategies requires writing programs, as in some cases these programs are complex and do not give satisfactory results. Therefore, simulation and experimentation were relied upon to determine the gain values of this designed controller. This method is fast and gives excellent results, as values were taken that gave excellent results in terms of current and PQ.

Table 1 represents a comparison between the designed regulator and some controllers found in the literature. This comparison gives a clear picture of the importance of this designed controller in the future as a promising solution in the industrial field.

This designed controller is used in the next section to overcome the problems of the DPC strategy of IG-SRLWT systems.

Proposed control approach

In this part, a new command based on the DPC approach is proposed based on the use of the proposed regulator represented in Eq. (13) and Fig. 2. This approach, designed to control powers, is used for IG, where the outputs of these controls are reference voltage values and their inputs are error powers, as shown in Fig. 3. According to Fig. 3, two controllers are used to control powers. The proposed DPC strategy based on the use of the controller

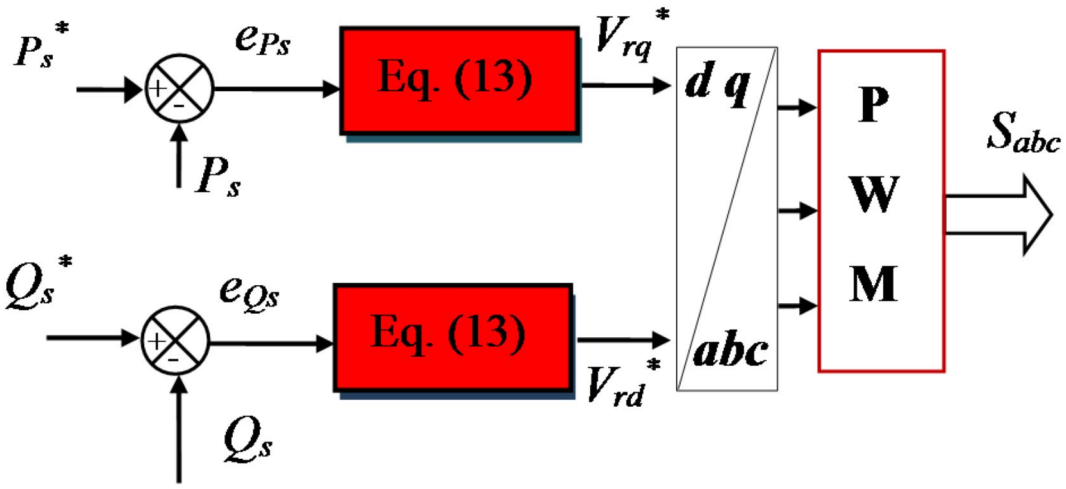

Fig. 3. Proposed control of RSC.

designed in the third section is used to control the RSC only to demonstrate the effectiveness, efficiency, and ability of this designed strategy to improve the quality of power and current without resorting to controlling the network inverter. The designed strategy is a modification of the traditional DPC strategy, where the switching table is compensated by the PWM strategy to generate the pulses needed to operate the machine inverter. Also, the controller designed in the third section is used to replace the traditional hysteresis controllers found in conventional control to generate the voltage reference values necessary to operate the inverter. These voltage reference values are generated from power errors.

In this designed strategy, the MPPT strategy is used to generate the reference value for the *Ps*, and thus the value of the current and torque becomes related to the shape of the WS change.

The general structure of the proposed strategy, which is based on the controller designed in the third section, is represented in Fig. 4. This proposed strategy relies on the use of power estimation to calculate the power error. Since the designed strategy is a development of the DPC strategy, the equations for estimating capabilities used in the DPC approach remain the same as in the designed strategy. This designed strategy differs from the works mentioned in the introduction section and scientific works[16,56,57].

According to the work done in[58], to estimate the capacity, the flux must first be estimated. As is known, flux estimation is linked to measuring voltage and stream. Using the Eqs. (14) and (15), the flux for the rotor and stator can be estimated.

$$\begin{cases} \Psi_{r\beta} = \int_0^t (V_r - R_r \times i_{r\beta})dt \\ \Psi_{r\alpha} = \int_0^t (V_r - R_r \times i_{r\alpha})dt \end{cases} \tag{14}$$

$$\begin{cases} \Psi_{s\beta} = \int_0^t (V_s - R_s \times i_{s\beta})dt \\ \Psi_{s\alpha} = \int_0^t (V_s - R_s \times i_{s\alpha})dt \end{cases} \tag{15}$$

Equation (16) represents the absolute value of the flux of the rotating and stator parts of the machine. This equation is used to implement the proposed approach in the MATLAB environment.

$$\begin{cases} |\Psi_s| = \sqrt{\left(\Psi_{s\beta}^2 + \Psi_{s\alpha}^2\right)} \\ |\Psi_r| = \sqrt{\left(\Psi_{r\beta}^2 + \Psi_{r\alpha}^2\right)} \end{cases} \tag{16}$$

The power estimation in this work is done using Eq. (17), where the estimation of these energies is used to calculate the energy error[59].

$$\begin{cases} Q_s = -\frac{3}{2}\left(\frac{V_s}{\sigma \times L_s} \times \Psi_{\beta r} - \frac{V_s \times L_m}{\sigma \times L_r \times L_s}\right) \\ P_s = -\frac{3}{2} V_s \times \Psi_{r\beta} \times \frac{L_m}{\sigma \times L_r \times L_s} \end{cases} \tag{17}$$

The energy error is determined according to Eq. (18), where the values of these errors are inputs to the proposed regulator. Using the MPPT approach makes the *Ps* reference related to the shape of the WS change. The reference value of the *Qs* is set to 0. So, the apparent power value in this case becomes the *Ps* and the power factor value is 1.

$$\begin{cases} e_{Ps} = -P_s + P_s^* \\ e_{Qs} = -Q_s + Q_s^* \end{cases} \tag{18}$$

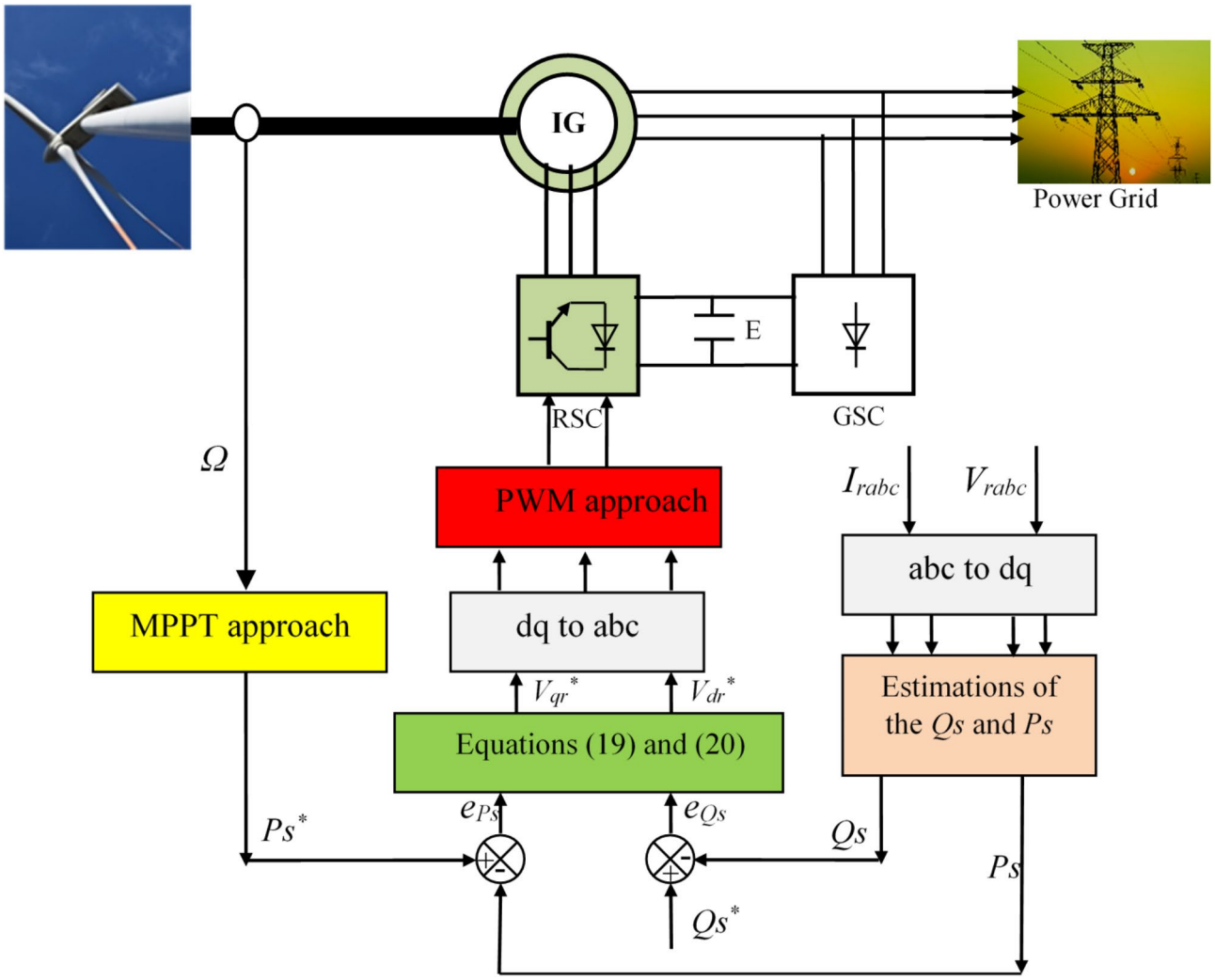

Fig. 4. Proposed power control system.

The suggested approach is a change and modification of the DPC approach, as they differ in terms of regulating the inverter and the controllers used to control powers. But they use the same estimation equations. So this designed approach maintains the simplicity and ease of realization found in the DPC approach and increases the robustness of the ES used.

Using available Equations (13), the proposed regulator used to control the IG capabilities can be expressed using Eqs. (19) and (20).

$$V_{qr}(t) = (K_1 e_{Ps}(t) + K_2 \frac{de_{Ps}(t)}{dt})(K_3 \int w_{qr}(t)\,dt) + K_1 e_{Ps}(t) \tag{19}$$

$$V_{dr}(t) = (K_1 e_{Qs}(t) + K_2 \frac{de_{Qs}(t)}{dt})(K_3 \int w_{dr}(t)\,dt) + K_1 e_{Qs}(t) \tag{20}$$

Where, K_1 to K_6 are the gains by which the DR of the controllers is adjusted.

The gain values of the controls used to control powers were calculated using the method of experimentation and simulation. This strategy was relied upon for its ease of use and obtaining values quickly without the need to write complex programs.

Using Eqs. (19) and (20), the proposed regulator for power control can be represented in Fig. 5.

To study the stability of the designed controller, the Bode curve or Lyapunov's theory can be used. Using these two methods allows us to verify the stability of the proposed controller. The use of Lyapunov's theorem depends on calculating the derivation of Lyapunov's function, where this method is a mathematical method based on calculation. Using the Bode curve to prove the stability of the designed controller is better than using Lyapunov's

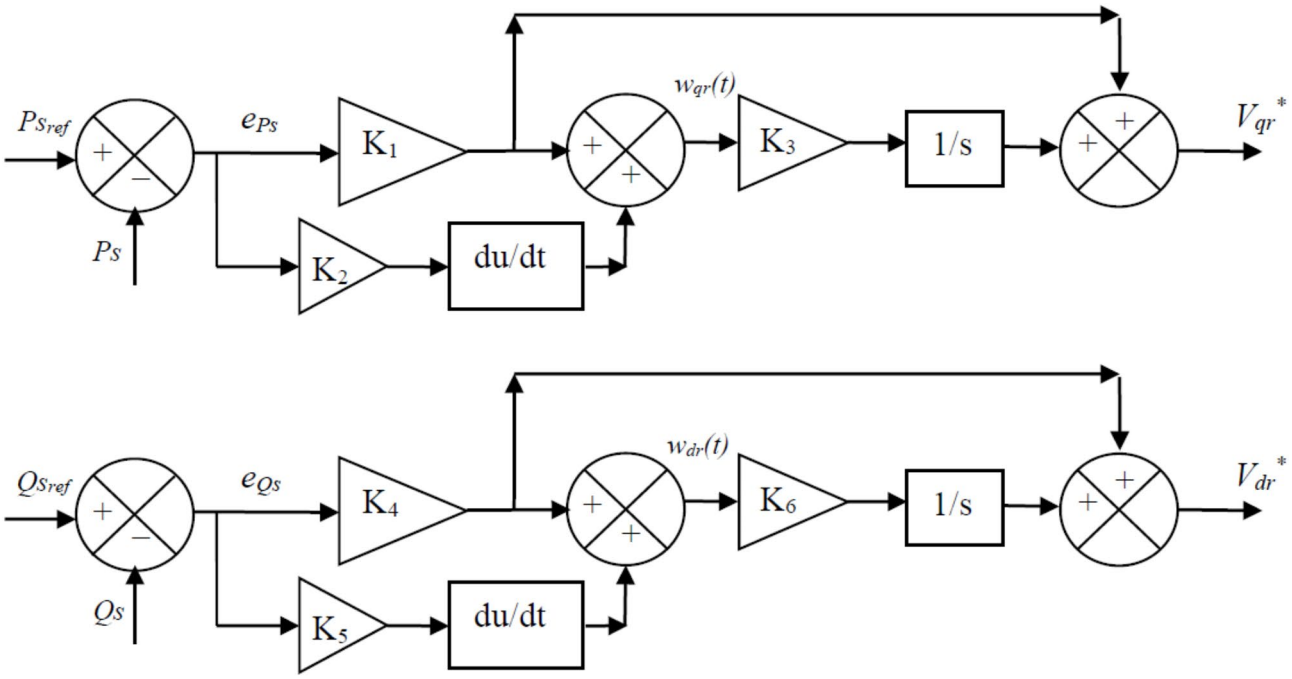

Fig. 5. Proposed *Ps* and *Qs* controllers.

theory, as this method does not depend on calculations such as the derivation calculation. The Budd curve is a simple and uncomplicated graphical method.

In this work, the Bode curve was relied upon to prove the stability of the designed controller. Figure 6 represents the Bode curve for the two controllers. Figure 6a represents the Bode curve of the PI regulator. The phase measured at 0 dB is -50°, so the phase margin is 50°. Also, the profit margin is positive. Since the phase margin is positive, this system based on the PI controller is stable.

Figure 6b represents the Bode curve of the designed controller. According to this figure, the phase measured at 0 dB has a negative value, and therefore the phase margin is a positive value. The gain at -180 degrees is negative, so the gain margin is positive. Since the phase margin is positive, this designed controller-based system is stable.

Table 2 represents a comparison of the proposed controller-based strategy with the DPC-PI strategy. In this table, the similarities and differences between these two controls are mentioned. Estimating capabilities and ease of completion are among the most prominent similarities between these two strategies used in this work. The differences between these two strategies lie in durability, performance, efficiency, and efficiency in improving PQ.

The designed strategy will be tested for validity and effectiveness in the next part, where it will be compared with the DPC-PI strategy. It is proposed to compare the obtained results with other works to prove the strength and effectiveness of the designed approach.

Results

In this section, the proposed approach is simulated using a 1500 W generator, where results are compared with the DPC-PI approach. The efficiency of the designed approach was studied in the case of using the MPPT strategy and not using it. Also, a comparison was made between the two controls in terms of reference tracking, THD, ripple reduction ratios, RT, SSE, and overshoot of IG power. The IG parameters are shown in Table 3.

Without MPPT technique test

In this test, the proposed approach is tested without using MPPT and comparing the results with the traditional strategy based on PI controller. The obtained results are represented in Figs. 7 and 8. The numerical results are represented in Table 4. From Fig. 7, it is noted that the powers follow the references well with a dynamic response in the case of using both controllers. Also, it is noted that there are ripples at the power level in both controllers. *Ps* has negative values and this is evidence of generating energy and sending it to the network. *Qs* has a fixed value equal to zero for the power factor to be equal to the value 1.

Figure 7c represents the stream as a function of time for both regulators. This stream has a sinusoidal shape with ripples, and its amplitude is linked to the values of *Ps*.

Figure 7d represents the change in power factor as a function of time for the two methods. It is noted that the value of this factor is constant and equal to one for the two controls, with the presence of ripples.

The THD of the stream for the two controllers can be known from Fig. 7e and f. From these two figures, the THD values were 0.69% and 1.57% for the new regulator and the PI regulator, respectively. Accordingly, the

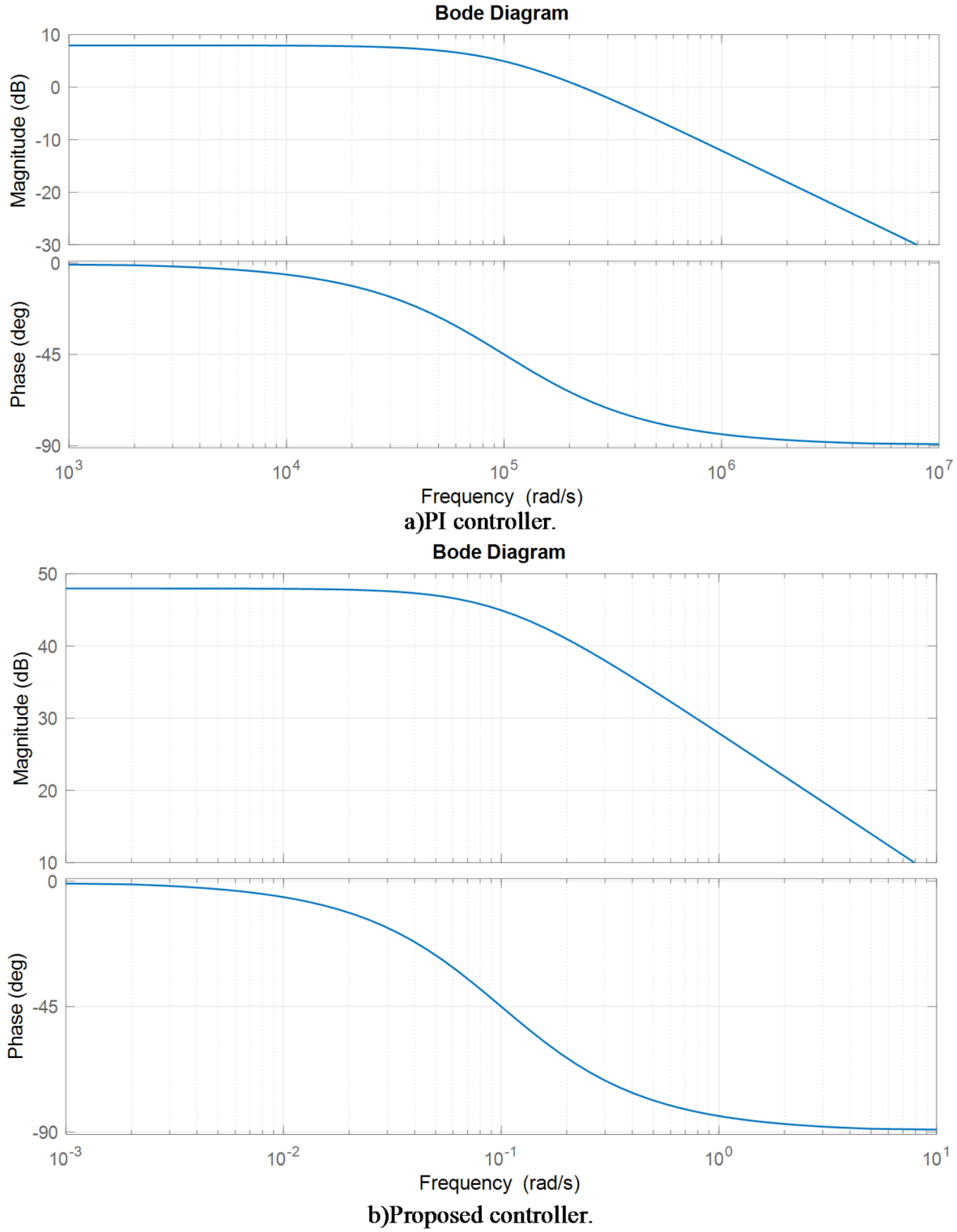

Fig. 6. Budd curve for both controls.

proposed regulator reduced the THD compared to the PI regulator, as this reduction was estimated at a rate of 56.05%. It is also noted that the designed controller provided an amplitude of the fundamental signal (50 Hz) equal to the PI controller. These results highlight the power of the controller designed to improve the quality of the current compared to using the PI controller.

In Fig. 8, a zoom of the graphical results of the first test is shown, where it is noted that the proposed regulator significantly reduced ripples for energy, power factor, and stream compared to the PI regulator. So, the fineness of energy and stream are high if the designed regulator is used compared to the PI regulator.

Features	DPC-PI	Proposed approach
Robustness	Low	High
MPPT	Yes	Yes
Power estimation	Yes	Yes
Switching table	No	No
Hysteresis controller	No	No
PI controller	Yes	No
Response dynamic	Very fast	Very fast
THD	Medium	Low
Power ripples	Medium	Low
Proposed controller	No	Yes
Stability	Stable	Stable

Table 2. Comparison between the designed approach and the DPC-PI approach.

Parameter	Values
R_s	1.18 mΩ
P_{sn}	1500 W
L_r	0.18 mH
L_m	0.17 mH
p	1
J	0.04 kg.m^2
L_s	0.20 mH
R_r	1.66 mΩ
f_r	0 mN.m/s
Vs	220/380 V
fs	50 Hz

Table 3. IG parameters.

Table 4 represents the numerical results for the designed strategy and the traditional strategy with reduction percentages for RT, spikes, SSE, and overshoot. Through these values, it is noted that the designed approach provided satisfactory results compared to the PI controller. The proposed controller reduces the values of ripple, SSE, and overshoot of *Ps* compared to the PI controller by percentages estimated at 69%, 54.40%, and 99.81%, respectively. In the case of *Qs*, the values of ripple, SSE, and overshoot were reduced by percentages estimated at 62.90%, 54.84%, and 88.37%, respectively, compared to the PI controller. These percentages indicate the effectiveness and strength of the approach designed to improve PQ characteristics compared to the PI approach. However, despite this performance, the designed controller provided unsatisfactory results in terms of RT to powers compared to the PI approach. It is noted that the PI approach reduced the RT by percentages estimated at 23.51% and 91.67% for both *Ps* and *Qs*, respectively, compared to the designed controller. The negativity of the proposed controller can be traced back to the values of gains, which can be overcome in the future by adding other strategies (merging) or using smart strategies to calculate the values of these gains.

With MPPT technique test

This test differs from the previous test, as the MPPT technique is used to study the effectiveness and strength of the proposed controller. This test is divided into two different tests, the first test in which the performance of the proposed approach is studied in the case of variable WS. The second test is to study the designed approach if the machine parameters change. The behavior of the proposed approach is compared to the PI controller in terms of ripple reduction ratios, RT, SSE, and overshoot of IG power. Also, the two strategies are compared in terms of THD value and tracking references.

Test 1: variable WS

In this test, the behavior of the proposed controller is studied using a variable WS, and the results are compared with a PI controller. The results of this test are included in Figs. 9 and 10. Also, the numerical results are listed in Table 5. The WS used in this test is listed in Fig. 9a. The powers continue to follow the references well (Fig. 9b and c) despite the change in the shape of the WS, with the fast DR of the two controllers. Also, the *Ps* keeps taking negative values, which is the same observation as in the without MPPT test. On the other hand, it is noted that the value of *Qs* is not affected by the change in WS, as it remains equal to the value 0 with the presence of fluctuations at the two control levels.

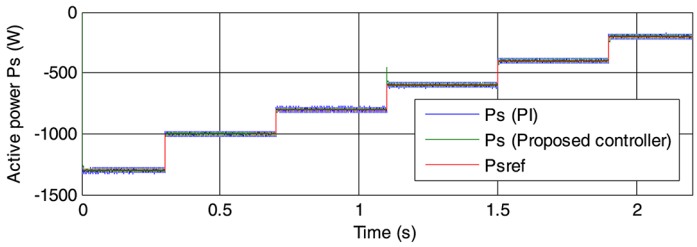

a)*Ps*.

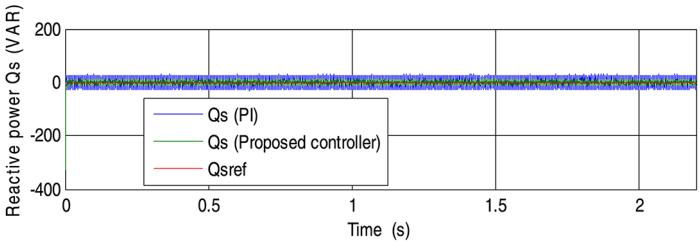

b)*Qs*.

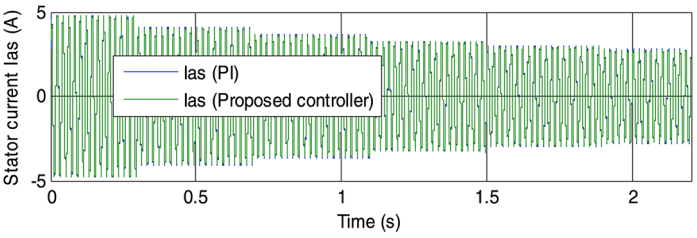

c)Stream

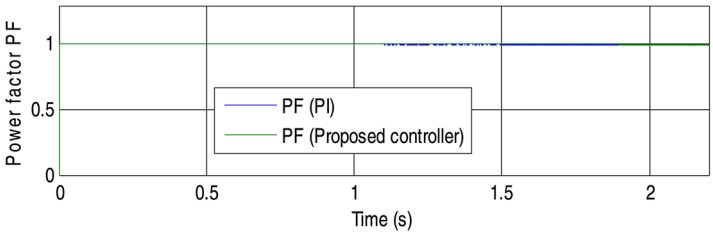

d)Power factor.

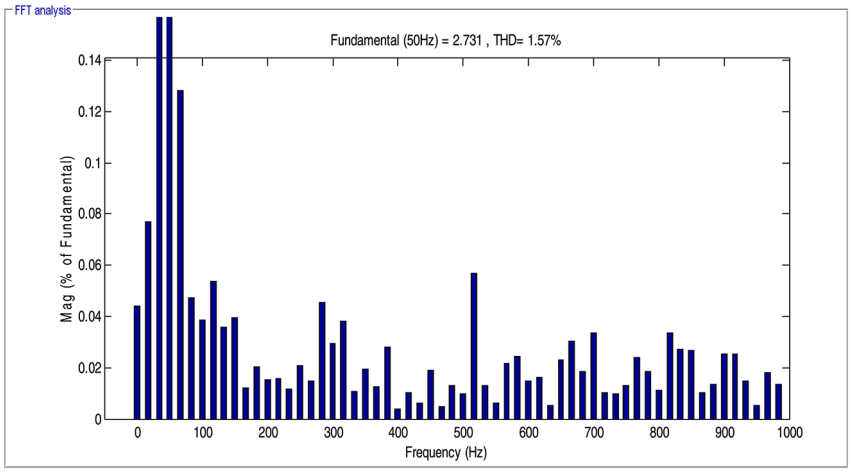

e)Stream THD (PI).

Fig. 7. Without MPPT technique test results.

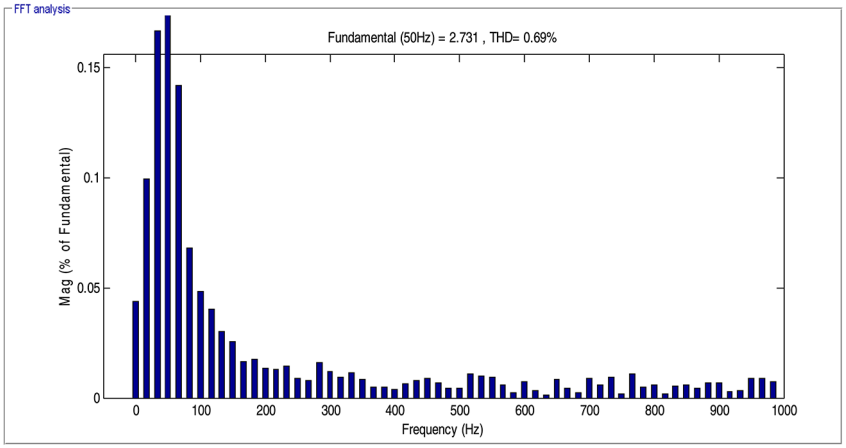

f)Current THD (Proposed controller).

Figure 7. (continued)

Figure 9d gives the change in current as a function of time for the two controllers, where despite the change in the shape of the WS, this stream remains sinusoidal for the two regulators. The value of this stream is linked to the change in the value of the *Ps*, and it is the same as the observations found in the first test.

Figure 9e represents the change in the power factor of the two controllers as a function of time. It is noted that the power factor does not change depending on the change in WS and its value is positive and constant. The power factor value remains equal to 1 for both controllers.

Figure 9f g represent the THD of both regulators. The THD values were 0.91% and 0.45% for the PI regulator and the designed regulator, respectively. So, the designed regulator reduced the THD significantly compared to the PI regulator, as this minimization was estimated at 50.55%. This ratio indicates that the designed regulator has a high competence in enhancing the stream fineness. It is also noted that the amplitude value of the fundamental signal (50 Hz) in this test is equal in the case of the two controllers, which is a good thing for the proposed controller.

In Fig. 10 a zoom of the graphical results of the variable WS test is shown. This figure shows that the proposed regulator minimized the undulations of stream, energy, and power factor well compared to the PI regulator. Therefore, the PQ is high in this test if the designed regulator is used.

Table 5 represents the reduction percentages obtained in the test using variable WS for the two controllers. This table gives the strengths and disadvantages of the proposed controller compared to the PI controller. The designed controller gave good values for ripple, SSE, and RT of *Ps*. The designed controller reduced the value of SSE, RT, and ripples of *Ps* by percentages estimated at 78.82%, 2.91%, and 61.70%, respectively, compared to the PI approach. The values of ripples and SSE of *Qs* were reduced by percentages estimated at 56.87% and 58.23%, respectively, compared to the PI controller. However, the designed controller provided unsatisfactory results in terms of overshoot and RT for *Qs* compared to the PI controller. PI controller reduced the overshoot value of IG power by percentages estimated at 81.82% and 92.67% for *Ps* and *Qs*, respectively, compared to the designed controller. Also, the PI controller gave a much better RT value than the controller designed with a ratio of 60.23%. These negatives can be attributed to the values of the gains. Other strategies can be added to the controller designed to overcome these drawbacks, such as the use of NNs.

Test 2: test of changing IG parameters

In this test, the IG parameters are changed to study the effectiveness and efficiency of the designed controller in improving the quality of power and current compared to the PI controller. The resistor values are multiplied by 2 and the machine coil values are divided by 2. In this test, the WS shown in Fig. 9a is used. The graphical results of this test are represented in Figs. 11 and 12. Also, the numerical results are listed in Table 6. According to Fig. 11, it is noted that despite the change in the IG parameters, the powers still follow the references well for the two controllers (Fig. 11a and b). Also, the current continues to take a sinusoidal shape, and its value changes according to the change in WS, which is the same as the observations found in the previous test (Fig. 11c). The power factor continues to take a value of 1 despite changing the IG parameters, as shown in Fig. 11d.

The THD value and fundamental signal (50 Hz) amplitude for two controllers are listed in Fig. 11e and f. The THD value was 1.33% and 0.6% for both the PI controller and the designed approach, respectively. Accordingly, the designed approach significantly reduced the THD value, as this reduction was estimated at a rate of 48.12% compared to the PI regulator. It is also noted that the amplitude value of the fundamental signal (50 Hz) is almost the same value for the two controllers, with an advantage for the proposed regulator, as its value was 3.354 A and 3.355 A for both the PI regulator and the designed controller, respectively. These results show the extent of the power of the proposed regulator, despite changing the IG parameters, to improve the quality of the current compared to the PI regulator.

In Fig. 12, a zoom of the graphical results of the test of changing IG parameters is shown, where it is noted that the proposed regulator significantly minimized fluctuations for power, power factor, and stream compared

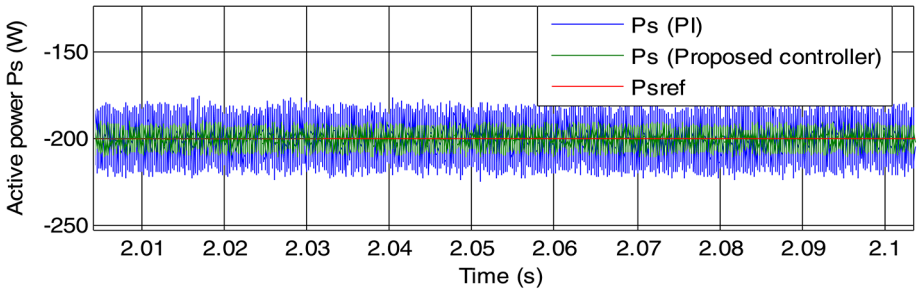

a)*Ps*.

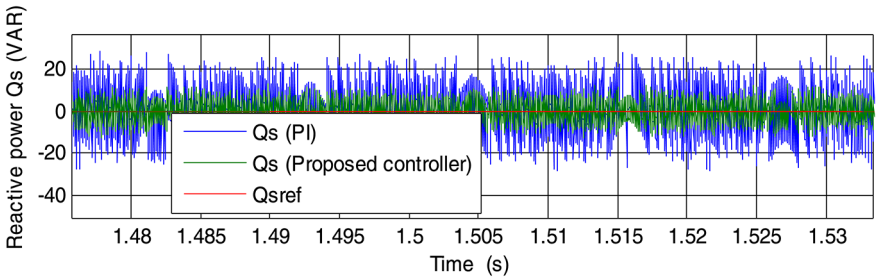

b)*Qs*.

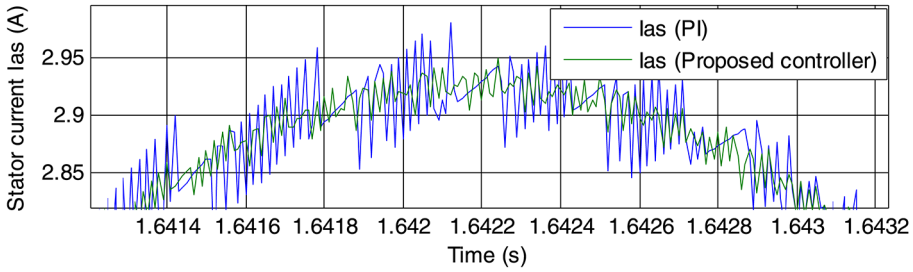

c)Stream.

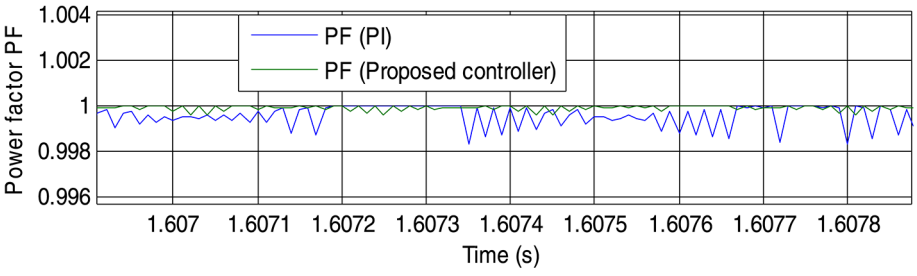

d)Power factor.

Fig. 8. Zoom (Without MPPT technique test).

to the PI regulator. So, the fineness of energy and stream are high if the designed regulator is used compared to the PI regulator.

Table 6 represents the reduction percentages for RT, ripples, SSE, and overshoot of IG power for the two controllers proposed in this work. Table 6 shows the superiority of the proposed regulator over the PI regulator in terms of ripple, SSE, and overshoot, and this appears through the calculated reduction ratios. In the case of *Ps*, the designed regulator reduced the ripple, SSE, and overshoot values by percentages estimated at 59.14%, 50.88%, and 77.14%, respectively, compared to the PI controller. In the case of *Qs*, the proposed regulator minimized the overshoot, fluctuations, and SSE values by ratios estimated at 72.22%, 54.77%, and 62.68%, respectively, compared to the PI regulator. The RT to power is much better when using a PI regulator than a designed regulator. Therefore, the RT is considered negative in this test for the designed regulator. The PI regulator reduced the RT compared to the designed regulator by rates estimated at 98.09% and 86.23% for both *Qs* and *Ps*, respectively. This negative can be overcome by using a GA strategy to calculate the gain values of the proposed controller or by combining this designed regulator with other techniques such as the FL approach.

		Qs (VAR)	Ps (W)
PI controller	Overshoot	6.70	321.85
	Fluctuations	58.70	50
	RT (ms)	0.404	0.540
	SSE	26.22	14.1
Proposed controller	Overshoot	0.779	0.60
	Fluctuations	21.78	15.50
	RT (ms)	4.85	0.706
	SSE	11.84	6.43
Improvement Ratios (%)	Overshoot	88.37	99.81
	Fluctuations	62.90	69
	RT (ms)	-91.67	-23.51
	SSE	54.84	54.40

Table 4. Numerical results of the case without MPPT approach.

Finally, the results obtained using the designed controller are compared with other methods in terms of RT, THD value, ripple, SSE, and overshoot. This comparison is included in Tables 7, 8, 9, 10 and 11.

Table 7 represents a comparison of the designed controller with other works in terms of RT to powers. It is noted that the controller has a fast DR compared to many existing strategies, which is a good thing that makes the designed controller an effective solution in other fields.

Table 8 represents a comparison of the designed controller with some papers in terms of the percentage of overshoot of powers. This table highlights the superiority of the designed controller over several scientific works in terms of the percentage of overshoot reduction of powers.

Table 9 represents a comparison of the proposed controller with other works in terms of the ripple reduction ratio for the powers. It is noted from this table that the designed controller has a greater reduction rate than several works, which highlights the extent of its strength and performance in improving PQ compared to several scientific works, which makes it one of the most prominent solutions in the future that can be relied upon.

Table 10 represents a comparison of the designed controller with other scientific works in terms of the percentage of reducing the SSE value of the powers. This table highlights that the designed controller has a greater reduction rate compared to several works, which highlights the extent of its strength and effectiveness.

Table 11 represents a comparison of the designed controller with scientific papers in terms of the THD value of the current. It is noted from this table that the THD value of the current is low in the case of using the designed controller compared to other scientific works. Therefore, the designed controller has a greater ability to improve the THD value compared to several tasks, which makes it a promising solution.

Conclusions

This work presents a new regulator to enhance the drawbacks of the DPC approach of IG-SRLWT, where the performance was compared with the PI approach. This proposed approach has several features that make it a promising solution in the future, such as simplicity, a small number of gains, and ease of realization. MATLAB was used to realize it and verify its robustness, efficiency, and competence using three different tests. The results obtained show the extent of the ability of this designed regulator to ameliorate the fineness of the stream by reducing the THD value compared to the PI regulator. The designed controller reduced the THD value by percentages estimated at 48.12%, 50.55%, and 56.05% in all tests compared to the PI controller. The designed controller reduced the ripple value of *Ps* and *Qs* by high percentages compared to the PI regulator, where the reduction percentages for *Ps* were 69%, 61.70%, and 59.14%. Reactive power reduction ratios were estimated at 62.90%, 56.87%, and 54.17% compared to the PI regulator. Therefore, the conclusions obtained from this work can be summarized in the following points:

- Overcoming DPC strategy problems.
- Overcoming the disadvantages of PI regulator.
- Reducing the overshoot value of *Ps* by percentages estimated at 77.14% and 88.37% compared to the PI controller.
- Reducing the SSE value of *Ps* by ratios estimated at 54.40%, 78.82%, and 50.88% in all tests compared to the PI controller.
- Reducing the SSE value of *Qs* by ratios estimated at 62.90%, 56.87%, and 54.17% in all tests compared to the PI regulator.
- Reducing the overshoot value of *Qs* by percentages estimated at 72.22% and 99.81% compared to the PI controller.
- The use of the designed regulator allows for increasing the durability of the studied energy system compared to the use of a PI regulator.
- Improving control stability compared to using a PI regulator.

These obtained results make the designed controller of great importance in the industrial field, as it can be relied upon in other fields such as traction and propulsion.

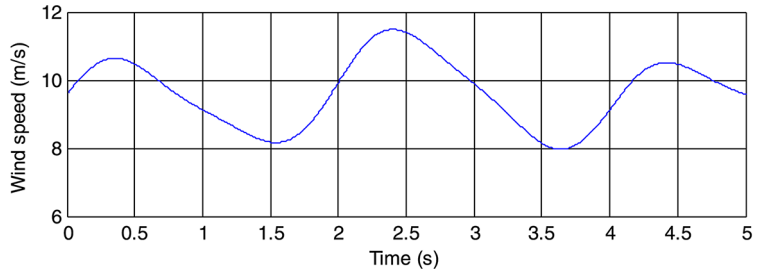

a)Variable WS profile.

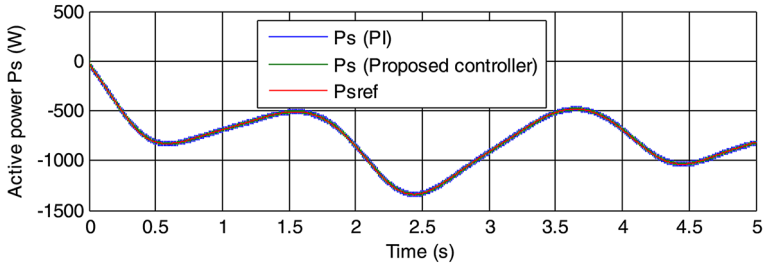

b)*Ps*.

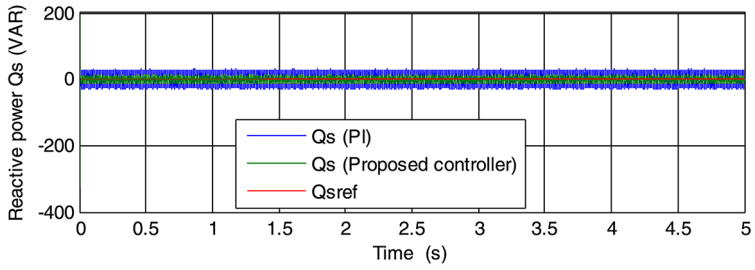

c)Qs

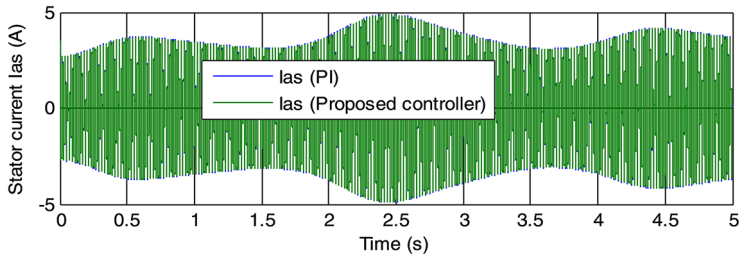

d)Stream

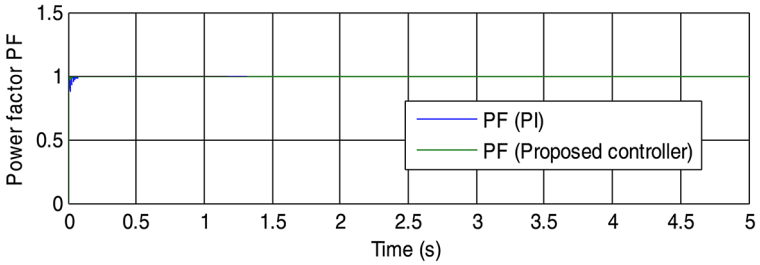

e)Power factor.

Fig. 9. Variable WS test results.

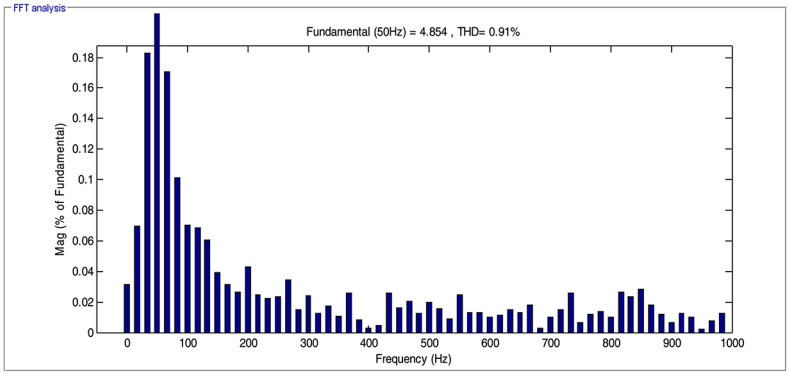

f) THD of stream (PI regulator).

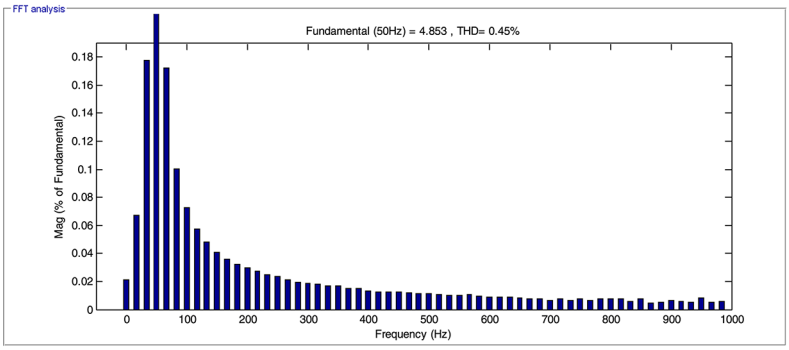

g) THD of current (Designed controller)

Figure 9. (continued)

This work has some limitations, such as implementation in MATLAB and using only one profile of WS variation to study the efficiency of the designed approach. Also, the effectiveness and impact of the designed controller were not studied in the event of a network malfunction. In the future, we will attempt to implement this controller experimentally and verify the validity of the results presented in this work. Also, try to apply the designed controller to the GSC and compare it with other controllers. In addition, an attempt will be made to integrate the designed controller with other strategies such as neural networks, SC, and fractional calculus to significantly improve performance and robustness.

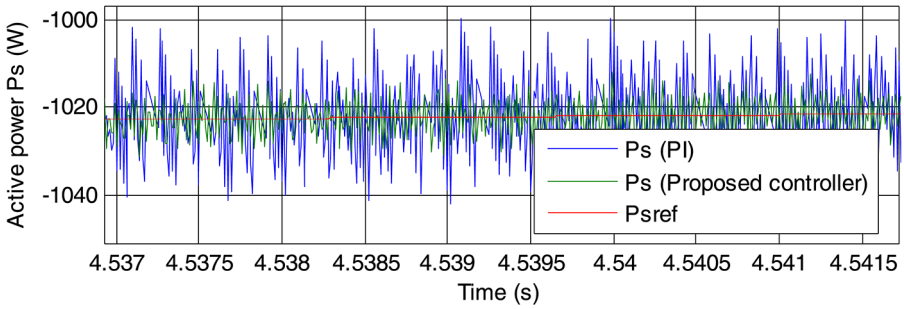

a)*Ps*.

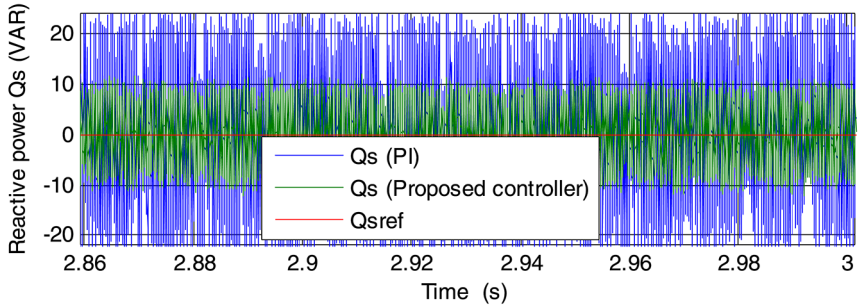

b)*Qs*.

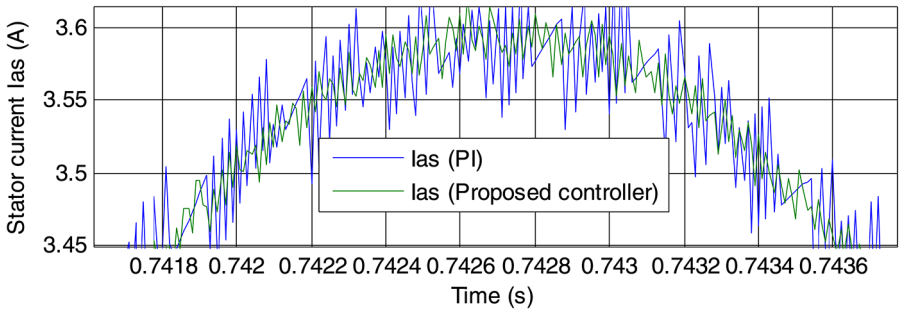

c)Stream

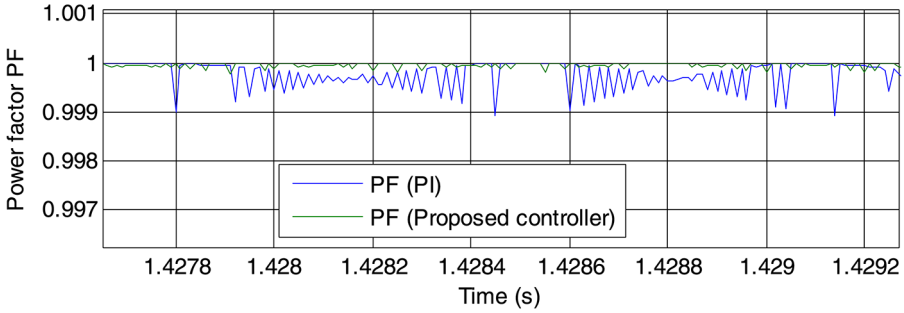

d)Power factor

Fig. 10. Zoom (Variable WS test).

		Ps (W)	Qs (VAR)
PI controller	Overshoot	05	14.42
	Fluctuations	47	52.40
	RT (ms)	0.103	0.105
	SSE	17	23.94
Proposed controller	Overshoot	50	196.70
	Fluctuations	18	22.60
	RT (ms)	0.100	0.264
	SSE	3.6	10
Improvement Ratios (%)	Overshoot	-81.82	-92.67
	Fluctuations	61.70	56.87
	RT (ms)	2.91	-60.23
	SSE	78.82	58.23

Table 5. Numerical results of test 1 (variable WS profile).

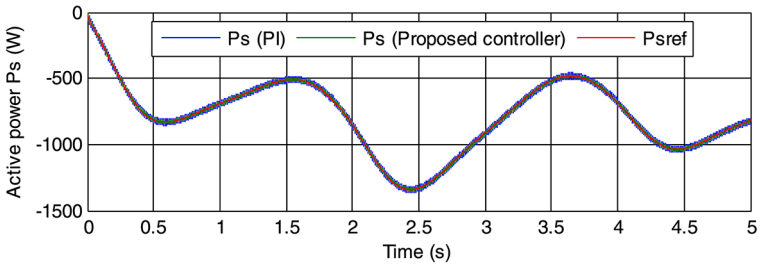

a)*Ps*.

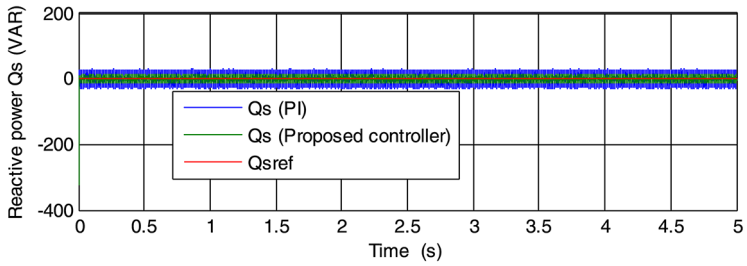

b)*Qs*.

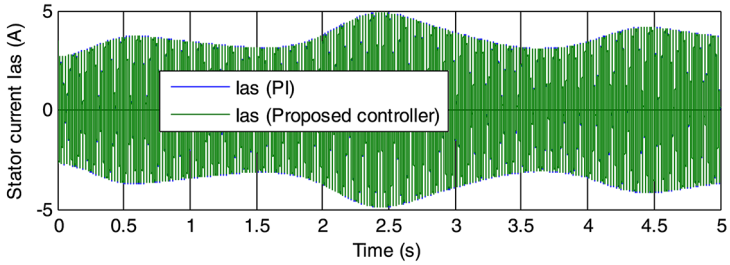

c)Stream

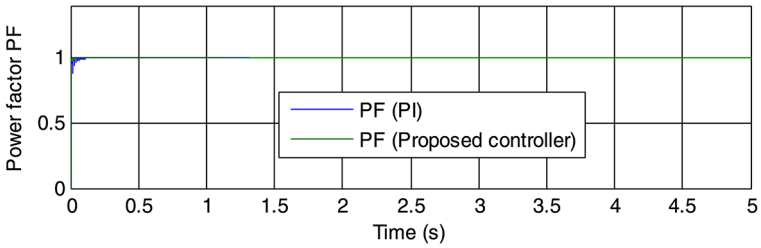

d)Power factor.

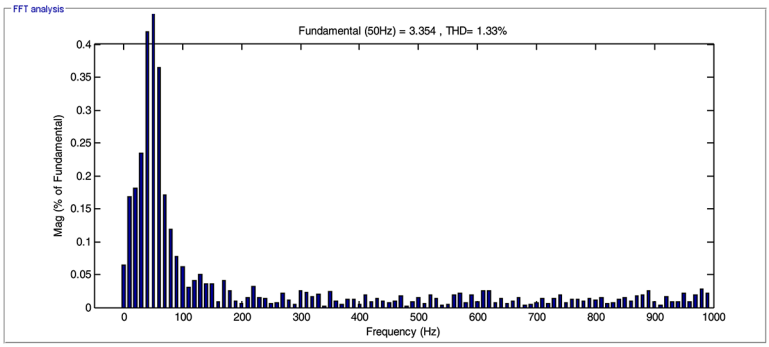

e)THD (PI controller).

Fig. 11. Robustness test results.

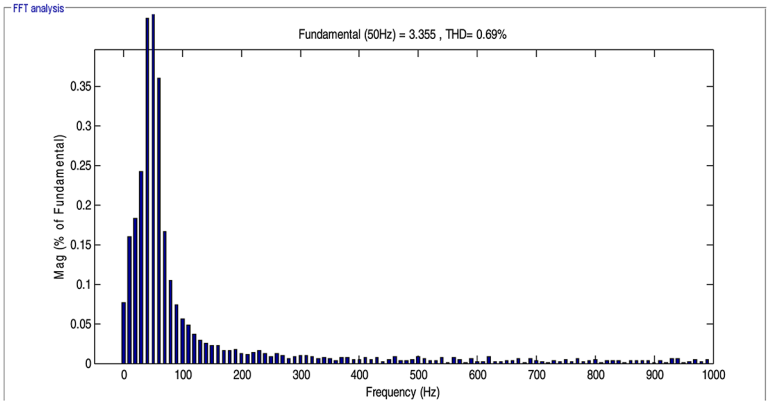

f)Current THD (Proposed regulator)

Figure 11. (continued)

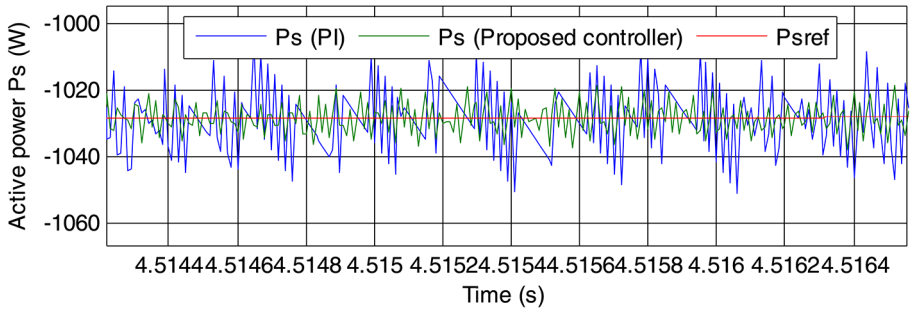

a)*Ps*.

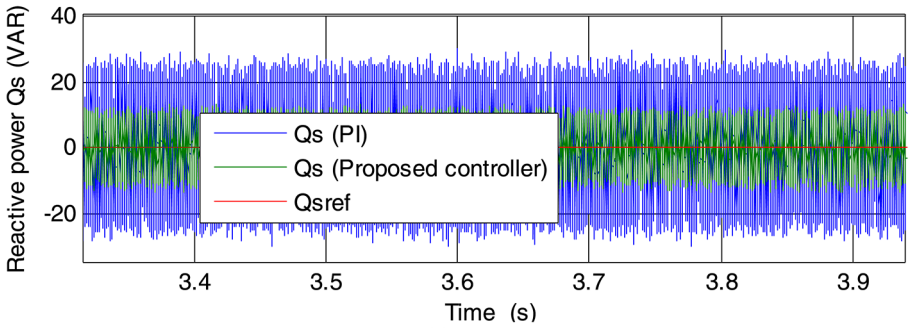

b)*Qs*.

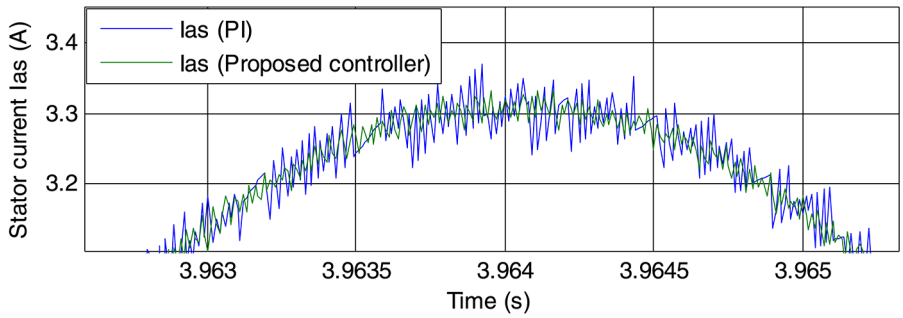

c)Stream.

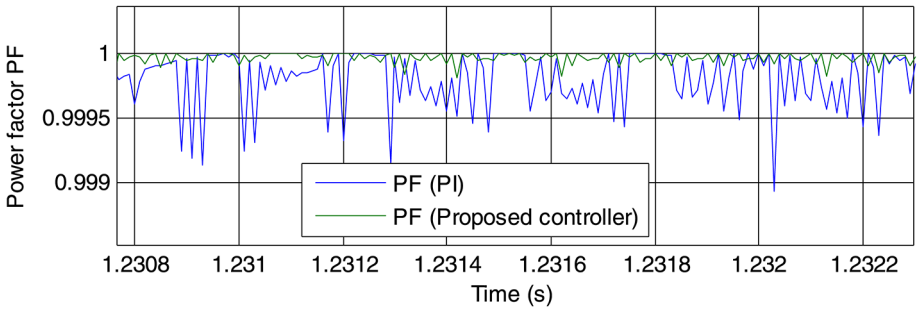

d)Power factor.

Fig. 12. Zoom (Test of changing IG parameters).

		Qs (VAR)	Ps (W)
PI controller	Overshoot	14.40	5.25
	Fluctuations	57.60	48.16
	RT (ms)	0.105	0.103
	SSE	25	17.02
Proposed controller	Overshoot	4	1.2
	Fluctuations	26.40	19.68
	RT (ms)	5.51	0.748
	SSE	9.33	8.36
Improvement ratios (%)	Overshoot	72.22	77.14
	Fluctuations	54.17	59.14
	RT (ms)	98.09	86.23
	SSE	62.68	50.88

Table 6. Numerical results of test 2 (test of changing IG parameters).

References		Power RT (ms)	
		Ps	Qs
[60]		15	80
[61]		33.8	34.5
[62]		5	4
[63]		-	28
[64]		2.2	0.90
[65]		1.50	0.80
[66]		1.78	8.50
[67]		1.70	1.85
		1.34	1.183
[68]		3.87	2.58
		1.29	0.46
[69]	DPC	17	18
	Nonlinear DPC approach	9	5
Designed controller		0.748	5.51
		0.264	0.100
		0.706	4.85

Table 7. A comparison between the designed controller and some papers in terms of RT.

References	Powers overshoot ratios (%)	
	Qs	Ps
[70]	48.38	73.87
	49.32	20.10
[71]	16.59	7.23
[72]	60.93	67.74
[73]	60.93	67.74
[74]	44.06	32.20
	22.77	32.49
[75]	65.90	70.96
	65.10	71.42
	67.44	70.31
Designed controller	72.22	77.14
	99.81	88.37

Table 8. Comparing the designed controller with some papers in terms of the minimization rates obtained for overshoot.

Ref.	Power fluctuation ratios (%)	
	Qs	Ps
[76]	36.93	22.95
[72]	46.93	28.57
[70]	50	44.50
	52.98	63.33
	50	48.18
[77]	54.25	56.66
	46.68	47.50
	50.74	50.41
[75]	66.93	60
	53.57	50
	69.10	61.66
[74]	12.02	10
	10.53	5.88
Proposed controller	62.90	69
	56.87	61.70
	54.17	59.14

Table 9. Comparison of power fluctuations minimization rates.

Ref.	SSE ratios (%)	
	Qs	Ps
[77]	78.44	45.83
	52.22	56.52
	48.75	87.50
[76]	36.93	35
[72]	42.14	47.57
[74]	38.32	50
	39.68	40
Proposed controller	54.84	54.40
	58.23	78.82
	62.68	50.88

Table 10. Comparison of SSE for IG power.

Current THD (%)	Ref.
2.15	[78]
3.13	[79]
6.70	[80]
2.40	
7.83	[81]
8.75	[82]
1.57	
3.70	[83]
4.88	[84]
4.19	
9.71	[85]
3.14	
1.19	[61]
4.59	[65]
18.51	
12	[86]
7.19	
0.69	**Proposed controller**
0.45	
0.69	

Table 11. Comparison of the results obtained with other approaches in terms of the current THD.

Data availability

Data available on request from the authors.The datasets used and/or analysed during the current study available from the corresponding author on reasonable request.In the event of communication, the fist author (Habib Benbouhenni, E-mail: habib.benbouhenni@enp-oran.dz) will respond to any inquiry or request.

Received: 29 October 2024; Accepted: 22 January 2025
Published online: 25 January 2025

References

1. Loulijat, A. et al. Application and comparison of a modified protection scheme utilizing a proportional–integral controller with a conventional design to enhance doubly fed induction generator wind farm operations during a balanced voltage dip. *Processes* **11**, 2834. https://doi.org/10.3390/pr11102834 (2023).
2. Soomro, M. et al. Performance improvement of grid-integrated doubly fed induction generator under asymmetrical and symmetrical faults. *Energies* **16**, 3350. https://doi.org/10.3390/en16083350 (2023).
3. Guediri, A., Hettiri, M. & Guediri, A. Modeling of a wind power system using the genetic algorithm based on a doubly fed induction generator for the supply of power to the electrical grid. *Processes* **11**, 952. https://doi.org/10.3390/pr11030952 (2023).
4. Mbukani, M. W. K., Gitau, M. N., Naidoo, R. & An SMC-MRAS speed estimator for sensor-less control of DFIG Systems in wind turbine applications. *Energies* **16**, 2633. https://doi.org/10.3390/en16062633 (2023).
5. Huang, J., Wang, H. & Wang, C. Passivity-based control of a doubly fed induction generator system under unbalanced grid voltage conditions. *Energies* **10**, 1139. https://doi.org/10.3390/en10081139 (2017).

6. Chojaa, H. et al. Nonlinear control strategies for enhancing the performance of DFIG-Based WECS under a real wind Profile. *Energies* **15**, 6650. https://doi.org/10.3390/en15186650 (2022).
7. Chakib, M., Tamou, N. & Ahmed, E. Contribution of variable speed wind turbine generator based on DFIG using ADRC and RST controllers to frequency regulation. *Int. J. Renew. Energy Res. -IJRER.* **11** (1), 320–331. https://doi.org/10.20508/ijrer.v11i1.11762.g8136 (2021).
8. Elnaghi, B. E. et al. The validation and implementation of the second-order adaptive fuzzy logic controller of a double-fed induction generator in an oscillating water column. *Electronics* **13**, 291. https://doi.org/10.3390/electronics13020291 (2024).
9. Loulijat, A. et al. Enhancement of LVRT ability of DFIG wind turbine by an improved protection scheme with a modified advanced nonlinear control loop. *Processes* **11**, 1417. https://doi.org/10.3390/pr11051417 (2023).
10. Iwański, G., Piwek, M. & Dauksha, G. Doubly fed induction machine-based DC voltage generator with reduced oscillations of Torque and output voltage. *Energies* **16**, 814. https://doi.org/10.3390/en16020814 (2023).
11. Sahri, Y. et al. Advanced fuzzy 12 DTC Control of Doubly Fed Induction Generator for Optimal Power Extraction in wind turbine system under Random wind conditions. *Sustainability* **13**, 11593. https://doi.org/10.3390/su132111593 (2021).
12. Yousefi-Talouki, A., Zalzar, S. & Pouresmaeil, E. Direct Power Control of Matrix Converter-Fed DFIG with fixed switching frequency. *Sustainability* **11**, 2604. https://doi.org/10.3390/su11092604 (2019).
13. Hichem, H., Chiheb, B. R. & Abderrahmen, Z. A. robust nonlinear controller approach of a wind energy conversion system based on a DFIG. in *IEEE 2nd International Conference on Signal, Control and Communication (SCC), Tunis, Tunisia*. 161–167. (2021). https://doi.org/10.1109/SCC53769.2021.9768376 (2021).
14. Sara, M., Ahmed, E., Tamou, N. & Badr, B. I. An efficient nonlinear backstepping controller approach of a wind energy conversion system based on a DFIG. *Int. J. Renew. Energy Research-IJRER.* **7** (4), 1520–1528. https://doi.org/10.20508/ijrer.v7i4.6112.g7192 (2017).
15. Khedher, A., Nihel, K. & Mohamed, F. M. Wind energy conversion system using DFIG controlled by backstepping and sliding mode strategies. *Int. J. Renew. Energy Research-IJRER.* **2** (3), 421–434. https://doi.org/10.20508/ijrer.v2i3.249.g6040 (2012).
16. Rayane, L. & Lekhchine, S. Fuzzy logic controller-based power control of DFIG based on wind energy systems. *Int. J. Smart Grid-ijSmartGrid.* **8** (1), 74–80. https://doi.org/10.20508/ijsmartgrid.v8i1.334.g346 (2024).
17. Mihir, M., & Bhinal, M Modified Rotor Flux Estimated Direct Torque Control for Double Fed Induction Generator. *Int. J. Renew. Energy Research-IJRER* **12**(1), 124–133. https://doi.org/10.20508/ijrer.v12i1.12615.g8380 (2022).
18. Boris, D., Bane, P., Dragan, M., Vladimir, K. & Djura, O. Artificial intelligence based vector control of induction generator without speed sensor for use in wind energy conversion system. *Int. J. Renew. Energy Research-IJRER.* **5** (1), 299–307. https://doi.org/10.20508/ijrer.v5i1.2030.g6498 (2015).
19. Hete, R. R. et al. Design and development of PI controller for DFIG grid integration using neural tuning method ensembled with dense plexus terminals. *Sci. Rep.* **14**, 7916. https://doi.org/10.1038/s41598-024-56904-7 (2024).
20. Sabzevari, K. et al. Low-voltage ride-through capability in a DFIG using FO-PID and RCO techniques under symmetrical and asymmetrical faults. *Sci. Rep.* **13**, 17534. https://doi.org/10.1038/s41598-023-44332-y (2023).
21. Ma, K., Wang, R., Nian, H., Wang, X. & Fan, W. Nonlinear model predictive control for doubly fed induction generator with uncertainties. *Appl. Sci.* **14**, 1818. https://doi.org/10.3390/app14051818 (2024).
22. Duong, M. Q., Leva, S., Mussetta, M. & Le, K. H. A comparative study on controllers for improving transient Stability of DFIG wind turbines during large disturbances. *Energies* **11**, 480. https://doi.org/10.3390/en11030480 (2018).
23. Singh, P. et al. Performance evaluation of grid-connected DFIG-based WECS with battery energy storage system under wind alterations using FOPID controller for RSC. *Mathematics* **11**, 2100. https://doi.org/10.3390/math11092100 (2023).
24. Tarek, B., Islam, A. S. & Doaa, K. I. Performance enhancement of doubly-fed induction generator-based-wind energy system. *Int. J. Renew. Energy Res. -IJRER.* **13** (1), 311–325. https://doi.org/10.20508/ijrer.v13i1.13649.g8685 (2023).
25. Loubna, B., Khafallah, M., Voyer, D., Mesbahi, A. & Bouragba, T. Nonlinear control based on fuzzy logic for a wind energy conversion system connected to the grid. *Int. J. Renew. Energy Research-IJRER.* **10** (1), 193–204. https://doi.org/10.20508/ijrer.v10i1.10381.g7855 (2020).
26. Dembri, R. et al. SSO optimized FOFPID regulator design for performance enhancement of doubly fed induction generator based wind turbine system. *Sci. Rep.* **14**, 28305. https://doi.org/10.1038/s41598-024-76457-z (2024).
27. Mohammadi Moghadam, H., Gheisarnejad, M., Yalsavar, M., Foroozan, H. & Khooban, M. H. A novel nonsingular terminal sliding mode control-based double interval Type-2 fuzzy systems: Real-time implementation. *Inventions* **6**, 40. https://doi.org/10.3390/inventions6020040 (2021).
28. Alhato, M. M., Ibrahim, M. N., Rezk, H., Bouallègue, S. & An Enhanced DC-Link Voltage Response for Wind-Driven Doubly Fed Induction Generator Using Adaptive Fuzzy Extended State Observer and Sliding Mode *Control Math.* **9**, 963. https://doi.org/10.3390/math9090963 (2021).
29. Ma, R., Han, Y. & Pan, W. Variable-Gain Super-Twisting Sliding Mode Damping Control of Series-Compensated DFIG-Based Wind Power System for SSCI Mitigation. *Energies* **14**, 382. https://doi.org/10.3390/en14020382 (2021).
30. Cheng, P., Wu, C., Ning, F., He, J. & Voltage Modulated, D. P. C. Strategy of DFIG using extended power theory under unbalanced grid voltage conditions. *Energies* **13**, 6077. https://doi.org/10.3390/en13226077 (2020).
31. Mazen Alhato, M., Bouallègue, S. & Rezk, H. Modeling and performance improvement of direct power control of doubly-fed induction generator based wind turbine through second-order sliding mode control approach. *Mathematics*. 8, (2012). https://doi.org/10.3390/math8112012 (2020).
32. Mazouz, F., Sebti, B., Ilhami, C. & DPC-SVM of DFIG Using Fuzzy Second Order Sliding Mode Approach. *Int. J. Smart Grid-Ijsmartgrid* **5**(4), 174–182. https://doi.org/10.20508/ijsmartgrid.v5i4.219.g178 (2021).
33. Mohammed, F., Ahmed, E., Mohamed, N. & Tamou, N. Control and optimization of a wind energy conversion system based on doubly-fed induction generator using nonlinear control strategies. *Int. J. Renew. Energy Research-IJRER.* **9** (1), 44–45. https://doi.org/10.20508/ijrer.v9i1.8812.g7619 (2019).
34. Sumanth, Y., Lakshminarasimman, L. & Sambasiva Rao, G. Optimal design of FoPID controller for DFIG based wind energy conversion system using Grey-Wolf optimization algorithm. *Int. J. Renew. Energy Research-IJRER.* **12** (4), 2111–2120. https://doi.org/10.20508/ijrer.v12i4.13446.g8594 (2022).
35. Samir, M., Mohamed, H., Nadir, K. & Selman, K. Neural network based field oriented control for doubly-Fed induction generator. *Int. J. Smart Grid–ijSmartGrid.* **2** (3), 183–187. https://doi.org/10.20508/ijsmartgrid.v2i3.18.g18 (2018).
36. Chakib, M. A comparative study of PI, RST and ADRC control strategies of a doubly fed induction generator based wind energy conversion system. *Int. J. Renew. Energy Research-IJRER.* **8** (2), 964–973. https://doi.org/10.20508/ijrer.v8i2.7645.g7383 (2018).
37. Sanjeev, K. G., Sundram, M. & Madhu, S. Performance enhancement of DFIG based grid connected SHPP using ANN controller. *Int. J. Renew. Energy Research-IJRER.* **9** (3), 1165–1179. https://doi.org/10.20508/ijrer.v9i3.9427.g7694 (2019).
38. Han, Y., Li, S. & Du, C. Adaptive higher-order sliding mode control of series-compensated DFIG-based wind farm for sub-synchronous control *Interact. Mitigation Energies* **13**, 5421. https://doi.org/10.3390/en13205421 (2020).
39. Chen, H. et al. Fractional-order PI control of DFIG-based tidal stream turbine. *J. Mar. Sci. Eng.* **8**, 309. https://doi.org/10.3390/jmse8050309 (2020).
40. Alhato, M. M. & Bouallègue, S. Direct power control optimization for doubly fed induction generator based wind turbine systems. *Math. Comput. Appl.* **24**, 77. https://doi.org/10.3390/mca24030077 (2019).

41. Sahar, A. N. et al. Optimal Power Management and Control of Hybrid Photovoltaic-Battery for Grid-Connected doubly-Fed induction generator based wind Energy Conversion System. *Int. J. Renew. Energy Research-IJRER.* **12** (1), 408–421. https://doi.org/10.20508/ijrer.v12i1.12770.g8422 (2022).
42. Adel, K., Nihel, K. & Mohamed, F. M. Wind energy conversion system using DFIG controlled by backstepping and sliding mode strategies. *Int. J. Renew. Energy Research-IJRER.* **2** (3), 421–430. https://doi.org/10.20508/ijrer.v2i3.249.g6040 (2012).
43. Hüseyin, C., Ahmet, D. & Yuksel, O. Investigation of dynamic behavior of double feed induction generator and permanent magnet synchronous generator wind turbines in failure conditions. *Int. J. Renew. Energy Res. -IJRER.* **11** (2), 721–729. https://doi.org/10.20508/ijrer.v11i2.11837.g8193 (2021).
44. Gasmi, H. et al. Fractional-order proportional-integral super twisting sliding mode controller for wind energy conversion system equipped with doubly fed induction generator. *J. Power Electron.* **22**, 1357–1373. https://doi.org/10.1007/s43236-022-00430-0 (2022).
45. Huseyin, C., Ahmet, D. & Yuksel O.Investigation of dynamic behaviourof double feed induction generator and permanent magnet synchronous generator wind turbines in failure conditions. *Int. J. Renew. Energy Research-IJRER.* **11** (2), 721–729. https://doi.org/10.20508/ijrer.v11i2.11837.g8193 (2021).
46. Tavakoli, S. M., Pourmina, M. A. & Zolghadri, M. R. Comparison between different DPC methods applied to DFIG wind turbines. *Int. J. Renew. Energy Research-IJRER.* **3** (2), 446–452. https://doi.org/10.20508/ijrer.v3i2.680.g6162 (2013).
47. Youcef, B., Djilani, B. A. & Comparison Study Between, S. V. M. and PWM Inverter in Sliding Mode Control of Active and Reactive Power Control of a DFIG for Variable Speed Wind Energy. *Int. J. Renew. Energy Research-IJRER* **2**(3), 471–476. https://doi.org/10.20508/ijrer.v2i3.269.g6047 (2012).
48. Mehta, M., & Bhinal, M. Modified rotor flux estimated direct torque control for double fed induction generator. *Int. J. Renew. Energy Research-IJRER* **12**(1), 124–133. https://doi.org/10.20508/ijrer.v12i1.12615.g8380 (2022).
49. Ch Rami, R., Naresh, K., Umapathi Reddy, P. & Sujatha, P. Control of DFIG based wind turbine with hybrid controllers. *Int. J. Renew. Energy Research-IJRER.* **10** (3), 1488–1500. https://doi.org/10.20508/ijrer.v10i3.11010.g8028 (2020).
50. Venktesh, M., Rishabh, D. S. & Premnath, G. An approach towards application of semiconductor electronics converter in autonomous DFIM based wind energy generation system: A review. *Int. J. Smart Grid-ijSmartGrid.* **3** (3), 152–162. https://doi.org/10.20508/ijsmartgrid.v3i3.69.g61 (2019).
51. Faisal, R. B., Subrata, K. S. & Sajal, K. D. Transient stabilization improvement of induction generator based power system using robust integral linear quadratic Gaussian approach. *Int. J. Smart Grid-ijSmartGrid.* **3** (2), 73–82. https://doi.org/10.20508/ijsmartgrid.v3i2.60.g48 (2019).
52. Mourad, Y. et al. Experimental validation of feedback PI controllers for multi-rotor wind energy conversion systems. *IEEE Access.* **12**, 7071–7088. https://doi.org/10.1109/ACCESS.2024.3351355 (2024).
53. Fatma, B., Abdelkarim, M., Achraf, A. & Lotfi, K. Coordinated Control of SMES and DVR for improving Fault ride-through capability of DFIG-based wind turbine. *Int. J. Renew. Energy Research-IJRER.* **12** (1), 359–371. https://doi.org/10.20508/ijrer.v12i1.12681.g8410 (2022).
54. Mohammed, F., Ahmed, E. & Tamou, N. Comparative Analysis between Robust SMC & Conventional PI controllers used in WECS based on DFIG. *Int. J. Renew. Energy Research-IJRER.* **7** (4), 2151–2161. https://doi.org/10.20508/ijrer.v7i4.6441.g7267 (2017).
55. Zahra, R., Mansour, R. & Mohammadreza, A. A. New Control Strategy based on reference values changing for enhancing LVRT capability of DFIG in wind farm. *Int. J. Renew. Energy Research-IJRER.* **9** (4), 1626–1637. https://doi.org/10.20508/ijrer.v9i4.9952.g7765 (2019).
56. Ben, A. J., Adel, K., & Mohamed, F. M. Speed-Sensorless, Wind Drive Based on DTC Using Sliding Mode Rotor Flux Observer. *Int. J. Renew. Energy Research-IJRER* **2**(4), 736–745. https://doi.org/10.20508/ijrer.v2i4.330.g6092 (2012).
57. Ahmed, M. Comparative study between direct and indirect vector control applied to a wind turbine equipped with a double-fed asynchronous machine article. *Int. J. Renew. Energy Research-IJRER.* **3** (1), 88–93. https://doi.org/10.20508/ijrer.v3i1.465.g6109 (2013).
58. Ghandehari, R., Ali, M. & Alireza Davari, S. A. New control algorithm method based on DPC to improve power quality of DFIG in unbalance grid voltage conditions. *Int. J. Renew. Energy Research-IJRER.* **8** (4), 2228–2238. https://doi.org/10.20508/ijrer.v8i4.8583.g7527 (2018).
59. Mohamed, N., Ahmed, E. & Tamou, N. Comparative analysis between PI & Backstepping Control Strategies of DFIG driven by wind turbine. *Int. J. Renew. Energy Research-IJRER.* **7** (3), 1307–1316. https://doi.org/10.20508/ijrer.v7i3.6066.g7163 (2017).
60. Alami, H. E & Mahfoud, M. et al. FPGA in the loop implementation for observer sliding mode control of DFIG-generators for wind turbines. *Electronics* **11** (1), 116. https://doi.org/10.3390/electronics11010116 (2022).
61. Echiheb, F. et al. Robust sliding-backstepping mode control of a wind system based on the DFIG generator. *Sci. Rep.* **12**, 11782. https://doi.org/10.1038/s41598-022-15960-7 (2022).
62. Ramos, C. J., Martins, A. P. & Carvalho, A. S. Rotor Current Controller with Voltage Harmonics Compensation for aDFIG Operating under Unbalanced and Distorted Stator Voltage. IECON 2007. 33rd Annual Conference of IEEE. 5–8 (2007).
63. Hamid, C. et al. Integral sliding mode control for DFIG based WECS with MPPT based on artificial neural network under a real wind profile. *Energy Rep.* **7**, 4809–4824. https://doi.org/10.1016/j.egyr.2021.07.066 (2021).
64. Wei, F., Zhang, X., Vilathgamuwa, D. M., Choi, S. S. & Wang, S. Mitigation of distorted and unbalanced stator voltage of stand-alone doubly fed induction generators using repetitive control technique. *IET Electron. Power Appl.* **7** (8), 654–663 (2013).
65. Xiong, P., Sun, D. & Backstepping-Based, D. P. C. Strategy of a wind turbine-driven DFIG under normal and harmonic grid voltage. *IEEE Trans. Power Electron.* **31** (6), 4216–4225. https://doi.org/10.1109/TPEL.2015.2477442 (2016).
66. Ardjal, A., Bettayeb, M., Mansouri, R. & Mehiri, A. Nonlinear synergetic control approach for dc-link voltage regulator of wind turbine DFIG connected to the grid. In *5th International Conference on Renewable Energy: Generation and Applications (ICREGA), Al Ain, United Arab Emirates*. 94–97. (2018). https://doi.org/10.1109/ICREGA.2018.8337639 (2018).
67. Yessef, M. et al. Experimental validation of feedback PI controllers for multi-rotor wind energy conversion systems. *IEEE Access.* **12**, 7071–7088. https://doi.org/10.1109/ACCESS.2024.3351355 (2024).
68. Yahdou, A. & Djilali, A. B. el al. Using neural network super-twisting sliding mode to improve power control of a dual-rotor wind turbine system in normal and unbalanced grid fault modes. International Journal of Circuit Theory and Applications. 0(0). (2024). https://doi.org/10.1002/cta.3960
69. Ibrahim, Y., Semmah, A. & Patrice, W. Neuro-second order sliding mode control of a DFIG based wind turbine system. *J. Electr. Electron. Eng.* **13** (1), 63–68 (2020).
70. Habib, B., Zellouma, D., Nicu, B. & Ilhami, C. A new PI(1 + PI) controller to mitigate power ripples of a variable-speed dual-rotor wind power system using direct power control. *Energy Rep.* **10**, 3580–3598. https://doi.org/10.1016/j.egyr.2023.10.007 (2023).
71. Sami, I., Ullah, S., Ali, Z., Ullah, N. & Ro, J. S. A super twisting fractional order terminal sliding mode control for DFIG-based wind energy conversion system. *Energies* **13**, 2158. https://doi.org/10.3390/en13092158 (2020).
72. Habib, B. et al. Backstepping control for multi-rotor wind power systems. *Majlesi J. Energy Manage.* **11** (4), 8–15 (2023). https://em.majlesi.info/index.php/em/article/view/493
73. Habib, B., Gasmi, H. & Colak, I. Comparative study of sliding mode control with synergetic control for rotor side inverter of the DFIG for multi-rotor wind power systems. *Majlesi J. Mechatron. Syst.* **11** (2), 29–37 (2023). https://ms.majlesi.info/index.php/ms/article/view/532

74. Yessef, M. et al. Real-time validation of intelligent super twisting sliding mode control for variable-speed DFIG using dSPACE 1104 board. *IEEE Access.* **12**, 31892–31915. https://doi.org/10.1109/ACCESS.2024.3367828 (2024).
75. Habib, B. et al. HIL Test Verification of PDPI Control of Induction Generator-Based Multi-Rotor Wind Turbine Systems. *Energy Sci. Eng.* **0**(0), 1–20. https://doi.org/10.1002/ese3.1976 (2024).
76. Habib, B., Gasmi, H., Colak, I., Nicu, B. & Phatiphat, T. Synergetic-PI controller based on genetic algorithm for DPC-PWM strategy of a multi-rotor wind power system. *Sci. Rep.* **13**, 13570. https://doi.org/10.1038/s41598-023-40870-7 (2023).
77. Habib, B., Bounadja, E., Gasmi, H., Nicu, B. & Ilhami, C. A new PD(1 + PI) direct power controller for the variable-speed multi-rotor wind power system driven doubly-fed asynchronous generator. *Energy Rep.* **8**, 15584–15594. https://doi.org/10.1016/j.egyr.2022.11.136 (2022).
78. Mahmoud, A. M., Echeikh, H. & Atif, I. Enhanced control technique for a sensor-less wind driven doubly fed induction generator for energy conversion purpose. *Energy Rep.* **7**, 5815–5833. https://doi.org/10.1016/j.egyr.2021.08.183 (2021).
79. Yahdou, A., Hemici, B. & Boudjema, Z. Second order sliding mode control of a dual-rotor wind turbine system by employing a matrix converter. *J. Electr. Eng.* **16**, 1–11 (2016).
80. Ayrira, W., Ourahoua, M., El Hassounia, B. & Haddib, A. Direct torque control improvement of a variable speed DFIG based on a fuzzy inference system. *Math. Comput. Simul.* **167**, 308–324. https://doi.org/10.1016/j.matcom.2018.05.014 (2020).
81. Said, M., Derouich, A., El Ouanjli, N. & Mahfoud, E. M. Enhancement of the Direct Torque Control by using Artificial Neuron Network for a Doubly Fed Induction Motor. Intelligent Systems with Applications. 13, 1–18. (2022). https://doi.org/10.1016/j.iswa.2022.20 0 060.
82. El Ouanjli, N. et al. Direct torque control of doubly fed induction motor using three-level NPC inverter. *Prot. Control Mod. Power Syst.* **4** (17), 1–9. https://doi.org/10.1186/s41601-019-0131-7 (2019).
83. Amrane, F., Chaiba, A., Babas, B. E. & Mekhilef, S. Design and implementation of high performance field oriented control for grid-connected doubly fed induction generator via hysteresis rotor current controller. *Rev. Sci. Techni -Electrotechn Et Energ.* **61** (4), 319–324 (2016).
84. Yusoff, N. A., Razali, A. M., Karim, K. A., Sutikno, T. & Jidin, A. A concept of virtual-flux direct power control of three-phase AC-DC converter. *Int. J. Power Electron. Drive Syst.* **8** (4), 1776–1784. https://doi.org/10.11591/ijpeds.v8i4.pp1776-1784 (2017).
85. Quan, Y., Hang, L., He, Y., Zhang, Y. & Multi-Resonant-Based Sliding Mode Control of DFIG-Based wind system under Unbalanced and Harmonic Network conditions. *Appl. Sci.* **9**, 1124. https://doi.org/10.3390/app9061124 (2019).
86. Mahfoud, S., Derouich, A., Iqbal, A. & El Ouanjli, N. Ant-colony optimization-direct torque control for a doubly fed induction motor: an experimental validation. *Energy Rep.* **8**, 81–98. https://doi.org/10.1016/j.egyr.2021.11.239 (2022).

Acknowledgements
This research was supported by King Khalid University, Research Project RGP.1/425/44.

Author contributions
Habib Benbouhenni: Writing – review & editing, Writing – original draft, Visualization, Validation, Supervision, Resources, Project administration, Methodology, Investigation, Formal analysis, Data curation, Conceptualization Nicu Bizon: Writing – review & editing, Visualization, Supervision, Methodology, Investigation, Formal analysis Ilhami Colak: Writing – review & editing, Visualization, Supervision, Methodology, Investigation, Formal analysis Z.M.S. Elbarbary: Writing – review & editing, Visualization, Supervision, Methodology, Investigation, Formal analysis Saad F. Al-Gahtani: Writing – review & editing, Visualization, Supervision, Methodology, Investigation, Formal analysis.

Funding
Not applicable.

Declarations

Competing interests
The authors declare no competing interests. Acknowledgement: This research was supported by King Khalid University, Research Project RGP.1/425/44.

Additional information
Supplementary Information The online version contains supplementary material available at https://doi.org/10.1038/s41598-025-87832-9.

Correspondence and requests for materials should be addressed to H.B.

Reprints and permissions information is available at www.nature.com/reprints.

Publisher's note Springer Nature remains neutral with regard to jurisdictional claims in published maps and institutional affiliations.